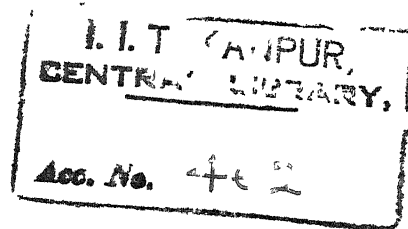


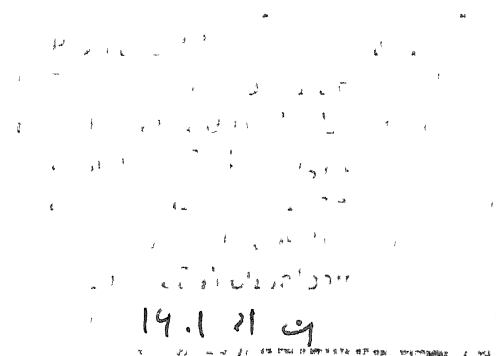
SOME STUDIES ON VIBROFLOATATION

A Thesis Submitted
In Partial Fulfilment of the Requirements
for the Degree of
MASTER OF TECHNOLOGY



BY
SHAMBHUPADA DASGUPTA

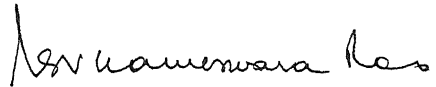
CE-1970-M-DIS-8



to the
DEPARTMENT OF CIVIL ENGINEERING
INDIAN INSTITUTE OF TECHNOLOGY KANPUR
DECEMBER, 1970

CERTIFICATE

Certified that this work "Some Studies on Vibroflotation" has been carried out by Sri Shambhupada Dasgupta under my supervision and the same has not been submitted elsewhere for a degree.



(N.S.V. KULKARNI R.O)
Assistant Professor,
Department of Civil Engineering
Indian Institute of Technology,
Kanpur

ACKNOWLEDGEMENT

The work reported herein, was performed under the guidance of Dr. N.S.V. Kameswara Rao, Assistant Professor of the Civil Engineering Department, Indian Institute of Technology, Kanpur.

The author wishes to express his deep and sincere gratitude to Dr. Kameswara Rao for his valuable guidance, keen interest in the work and encouragement throughout the preparation of this dissertation.

The author is very much thankful to Mr. S.V. Kapoor and Mr. Saini for their invaluable help in conducting experiments.

Thanks to Mr. K.V. Lakshmidhar and Mr. R.P. Trivedi of Soil Mechanics Laboratory for their help during the fabrication of the necessary equipment and the operation of electronic equipment during the experimentation.

To Mr. S.N. Pandey goes my thanks not only for his accurate typing but also for his valuable suggestions.

The author, again, wishes to express his sincere gratitude to the faculty members and staffs of the Civil Engineering Department for their invaluable co-operation.

CONTENTS

	Page
ACKNOWLEDGEMENTS ...	1
* TABLE OF CONTENTS ...	11
LIST OF ILLUSTRATIONS ...	1v
NOTATIONS ...	vi
SYNOPSIS ...	1x
 CHAPTER I INTRODUCTION	
1.1 General ...	1
1.2 Importance and Purpose of the Study of Liquefaction Phenomenon	2
1.3 Scope of this Investigation	4
 CHAPTER II A GENERAL DISCUSSION AND LITERATURE REVIEW	
2.1 Introduction ...	8
2.2 Qualitative Approach ...	9
2.3 Analysis of Vibro-floatation	13
2.4 General Discussion and Development of the Present Investigation	17
2.5 Accelerated Motion of Sphere in a Fluid	19
 CHAPTER III ANALYTICAL APPROACH	
3.1 Introduction ...	22
3.2 Accelerated Motion of a Sphere in an Oscillating Fluid.	22
3.3 Numerical Solution for the Governing Equation	28
3.4 Runge-Kutta Method of Integration	29
3.5 Comparison of the Solutions Obtained with the Existing Results	31
3.6 Discussion ...	33

		Page
CHAPTER IV	EXPERIMENTAL SETUP	
4.1	Objective	37
4.2	Instrumentation	37
4.3	Testing Procedures	42
CHAPTER V	TEST RESULTS	
5.1	Test Data	44
5.2	Soil Behaviour	44
5.3	Vibro-viscosity	45
5.4	Visicorder Records	50
CHAPTER VI	GENERAL DISCUSSION AND CONCLUSIONS	53
	REFERENCES	56
APPENDIX - I	Flow Chart for the Numerical Integration Procedure	61
APPENDIX - II	Derivation of the Basic Equation.	63
TABLES	
5.1	Variation of vibro-viscosity with frequency and superimposed load	50

LIST OF ILLUSTRATIONS

FIGURE		Page
2.1	Variation of internal friction with amplitude of vibration	68
2.2	Variation of internal friction with frequency of vibration	68
2.3	Effect of vibration on varying sand grain size.	68
2.4	Effect of acceleration on vibro-viscosity	69
2.5	Variation of viscosity and internal friction with water content	69
2.6	Variation of void ratio with acceleration of vibration	70
2.7	Probability of liquefaction of saturated sand	70
3.1	Comparison of proposed solution with the existing results	71
3.2	Stability check of the numerical integration	71
3.3 to 3.10	Solutions of the governing equation with varying the parameters involved	72
3.12 to 3.13	Check of reliability of the integration technique	78
3.14	Check of Konig's result	79
4.1	Instrument-interconnection diagram	80
4.2	Shaker schematic diagram	81
4.3	Aschematic diagram of the experimental setup	82

FIGURE

5.1 to 5.11	Experimental results	83
5.12	Grain size analysis	87
5.13	Variation of vibro-viscosity with frequency	88
5.14 to 5.15	Experimental results with the theoretical solutions	89
5.16 to 5.18	Displacement-time responses	90
5.19	Acceleration-time responses	93

NOTATIONS

The following symbols have been adopted for use in this dissertation:

A	=	Viscous drag coefficient;
a, \dot{a}, \ddot{a}	=	Position, velocity and acceleration co-ordinate;
a_0	=	Amplitude of soil vibration;
d	=	Diameter of the sphere;
e	=	Void ratio of the soil;
e_{\max}	=	Void ratio at the loosest state of soil;
e_{\min}	=	Minimum limit of void ratio of the soil;
F	=	Superimposed load on the sphere;
f	=	Frequency of soil vibration;
G_s	=	Specific gravity of soil;
g	=	Acceleration due to gravity;
k	=	Added mass coefficient of sphere;
L	=	A characteristic length;
M	=	A non-dimensional constant, defined in Eq.(3.6);
m_s	=	Mass of the sphere;
m_f	=	Mass of the volume of soil displaced by the sphere;
N	=	A non-dimensional constant, defined in Eq. (3.6);
N_s	=	A dimensionless constant equivalent to Stokes number;
P, Q	=	Non-dimensional constants, defined in Eq. (3.6);
R	=	Density ratio of sphere to soil mass;
RA	=	Ratio of amplitude of soil vibration to the characteristic length;

RB	=	Ratio of acceleration of gravity to soil acceleration
r	=	Radius of the sphere;
S	=	A non-dimensional constant, defined in Eq.(3.6);
T	=	Dimensionless time factor;
t	=	Time;
V	=	Ratio of the non-dimensional velocity to the Stokes terminal velocity;
V_t	=	Stokes terminal velocity;
v	=	Steady velocity of the sphere;
w	=	Angular velocity of soil motion
X, \dot{X}, \ddot{X}	=	Dimensionless displacement, velocity and acceleration of the sphere, respectively;
x, \dot{x}, \ddot{x}	=	Position, velocity and acceleration co-ordinate of the sphere, respectively;
x_0	=	Half amplitude of the sphere motion;
Z	=	Dimensionless velocity of the sphere,

Greek Letters:

β	=	A coefficient to determine the effect of vibration;
δ	=	Characteristic value of effect of vibration;
γ_s	=	Unit weight of sphere;
γ_f	=	Unit weight of soil
η	=	Ratio of acceleration of soil vibration to the acceleration due to gravity;
η_0	=	Threshold of vibro-viscous state of soil;
ρ_s	=	Mass density of the sphere;
ρ_f	=	Mass density of soil
τ	=	An interval, $0 \leq \tau \leq t$

- μ = Coefficient of vibro-viscosity;
- ν = Kinematic viscosity of soil;
- ϕ = Angle of internal friction of soil;
- ϕ_{st} = Angle of internal friction of soil without vibration;
- ϕ_{∞} = Limit value of the angle of internal friction of soil due to vibration;
- ψ = Stokes current function.

SYNOPSIS

The behaviour of Foundations, such as footings, piles etc. which are supported by the soil medium, when subjected to intense vibrations either due to earthquakes (natural or artificial), and other agencies, is an important aspect in Soil Mechanics. The soil when subjected to vibrations tends to liquefy and behaves like a fluid as the intensity of vibration increases. The coefficient of viscosity of the fluidised soil medium (which is called vibro viscosity) is a significant property which influences the soil-structure interaction. Hence, to have a feel for the behaviour of structures founded on such a soil environment analytical and experimental studies have been conducted in this investigation. ✓

In the study described here in, the vibroviscosity of a loose-fine grained-cohesionless unsaturated soil deposit subjected to intense vibration and its dependence on various soil parameters as well as the vibration characteristics has been studied experimentally and a mathematical relationship is established. ✓

On liquefaction the soil behaves like a fluid and hence the following Fluid Mechanics concepts have been brought here to determine the soil characteristics as mentioned earlier. Stokes performed an approximate solution of the Navier-Stokes equations for a stationary fluid which several

investigators have attempted to verify. Carstens solved the problem for an oscillating fluid making several simplifying assumptions.

In accelerated motion of a submerged body, the fluid being accelerated exerts a force on the body. This force is represented by a product of the body acceleration and the fictitious mass called the virtual mass. Usually the virtual mass is either neglected or its magnitude is determined from the irrotation-solutions for rectilinear motion. In the present analysis all the forces have been taken into account and solutions have been obtained using Runge-Kutta integration technique.

Laboratory tests have been conducted on the motion of a sphere in a soil medium subjected to vibrations. The vibro viscosity of the soil has been obtained using the above mentioned analysis of the accelerated motion of a sphere in an oscillating fluid and has been compared with the values obtained from Stokes classical solution. The effect of grain size of the soil, operating frequency, load superimposed on the sphere etc. have been studied. Results have been graphically presented and are compared with existing solutions.

CHAPTER - I

INTRODUCTION

1.1 General:

Static investigations of non-cohesive soil show high resistance to deformation even if it ~~is~~ saturated and having low values of porosity. This is verified by field and laboratory tests i.e. load test, consolidometer tests etc. If any soil (cohesive or non-cohesive) is subjected to dynamic loads, the resistance to external loads decreases considerably. This is verified by plunging vibrators, vibrating piles, pipes or cylinders with considerable diameter into the soil.

The settlement of vibrating foundations or other structural elements are predominant in loose non-cohesive soils. Loose fine sands whether saturated or not show a loss of strength under the action of dynamic loads. The loads may come from various sources e.g. Earthquakes, Nuclear-blasts, machine foundations etc. The loss of strength results due to the changes in dissipative properties of soil e.g. forces of internal dry and viscous friction, forces of cohesion (which determine the initial resistance of soil to shear), forces of external friction, hydrodynamic properties e.g. the coefficient of permeability and the pore water pressure and elastic and plastic characteristics such as Young's Modulus, the modulus of shear and the limits of elasticity and of plasticity.

It was also found that due to vibration sandy fills and loose silty and clayey soils get compacted at first and if vibration intensity is increased more and more they lose their resistance to shear and at a certain stage will reach when their mechanical properties are close to those of viscous liquids than of solids. The phenomenon is called vibrofloatation. The stage at which the soil behaves like a high viscous fluid is termed as liquefied stage and the phenomenon is called liquefaction. This phenomenon of liquefaction results in the failure of earth structures and foundations. This may include sliding of quay walls, settlement of earthen embankments and filling up of mines with liquefied soil.

1.2 Importance and Purpose of the Study of Liquefaction Phenomenon:

1.2.1 Studies in India:

Importance of such studies is being felt in India because of the increase in construction activities in the seismically active zones. The Banas River Dam in Gujarat and Oshana Dam in U.P. are two typical examples where the foundations are of loose sand and the dams are located in the seismically active zones.

1.2.2 Importance from Field Evidences:

During earthquakes, sand volcanoes and eruption of water and soil from the ground are often observed and especially in the NIIGATA²³ earthquake of June 16, 1964, extensive damage

to the structures occurred as a result of decrease in bearing capacity of soil. This decrease in bearing capacity of soil is due to two phenomena, one of which is liquefaction of the soil which extends from the ground surface to some depth and the other is the loosening of the soil due to upward flow of water which resulted from liquefaction of the soil at some distance below the ground surface.

Another typical example of liquefaction from earthquake is TOKACHI³⁹ earthquake of 1968. Due to this earthquake saturated sands underwent complete liquefaction at NANAEHAMA BEACH, HAKODATE, HOKKAIDO at coastal stretch of newly built hydraulic fill, resulting in numerous sand volcanoes of 2 cms to 50 cms high and the craters were 2 cms to 130 cms in diameter, grain sizes were ranging from 0.002 mm to 0.2 mm. It was observed at a plant in HACHINOHE city where a part of the building site was located on the back-fill sand prior to construction of the plant buildings, the loose sand was densified by Vibrofloatation and the main building was supported on the point bearing piles, the structure on piles and those on virgin ground showed little damage, whereas the improved back-fill area underwent complete liquefaction causing many structures to tilt settle or float up.

In Ohsaki's^{23,24} opinion the following five items are the conditions under which the ground would liquefy during an earthquake of a considerable intensity, resulting in heavy

damage to structures;

- 1) Most of the soil from the ground surface down to a depth of 15 to 20 m consists of sands,
- 2) It is submerged under the ground water table,
- 3) Its age of deposition is young ,
- 4) It consists of pure, uniform sands of medium grain size, i.e. i) the content of silt and/or clay is less than 10 percent, ii) its 60 percent grain size is in the range of 0.2 to 2.0 mm, and iii) its coefficient of uniformity is less than 5.
- 5) Its compactness is loose and N-values of the S.P.T. are smaller than the critical value represented by $N_{cr} = 2Z$, in which Z denotes a depth in metres.

During the earthquake of New Madrid in 1811, as quoted by Karl Terzaghi³⁷, many slopes failed. Reason he gave was that the submerged masses of loose sand might under the impact of an earthquake shock, temporarily assumed the character of suspension which flowed like a viscous liquid.

1.3 Scope of this Investigation:

The studies of Vibro floatation, particularly on liquefaction, were limited to saturated or partially saturated soils in English countries, although these tests were conducted for dry soils, in addition, by the Russians.

Liquefaction studies, which the present work deals, in particular, are being limited within the dry sands having very fine to medium grain size subjected to steady state vertical vibration. It has been tried to present a mathematical model for the sinking behaviour of a sphere. It has been assumed that the soil flows like a viscous fluid with having very high viscous resistance, coefficient of which is known as vibro-viscosity. An expression is developed for the accelerated motion of spherical bodies in an oscillating fluid, assuming the existence of a single degree-of-freedom system.

The phenomenon of liquefaction results from the increase in pore water pressure and consequent reduction in shear strength, as it is being noted by several Investigators. Liquefaction studies in dry fine grained soils is important due to the fact that the surface of the ground is more vulnerable to liquefaction compared to the depth below. In finegrained soils the reduction in shear strength may be upto cent percent and as this strength reduces the soil behaves more and more like a viscous fluid.

The phenomenon of liquefaction of the fine sands have been studied both in the laboratory and in the field by various Investigators for moist soil. The factors that affect the liquefaction are:

- i) Grain Size Characteristics
- ii) Density of deposit

- iii) Surcharge weight
- iv) Vibration characteristics
- v) Location of drainage
- vi) Dimension of deposit etc.

The vibration characteristics used here will be of steady state motion of simple Harmonic type, the other type, usually used, may be repeated loading. The soil property, at its liquefied stage, is being characterized by the coefficient of vibro-viscosity, and the present work will be to study the affect of frequency, amplitude and acceleration on the coefficient of vibro-viscosity, both theoretically and experimentally. This study will ultimately reveal the parameters which affect the viscous property of the soil continuum on vibrofloatation.

Chapter II concentrates on the review of past literature in the light of the present Investigation.

Chapter III deals with the theoretical formulation of the subject matter and solutions. All theoretical derivations and results are presented in this Chapter.

Chapter IV describes the experimental setup. A brief description of the each component and limitation of the experimental derivations etc. are reported here.

Chapter V deals with the analysis of test results and its correlation with the theoretical findings and comments on the results performed.

The last chapter (Chapter VI) deals mainly with a general discussion, scope for further studies, comments on the theoretical as well as experimental findings.

CHAPTER II

A GENERAL DISCUSSION AND LITERATURE REVIEW

2.1 Introduction:

Pokrovsky (1934) and associates, as quoted by Barkan¹ were the first to observe a decrease in strength of dry and moist sands under vibrations. They showed that the coefficient of internal friction depends on the Kinetic energy of vibration, as the energy increases, the coefficient decreases, approaching a value 25 to 30 percent smaller than that observed before vibration.

In English known countries probably the first attempt to delineate conditions under which a considerable reduction in shear strength of cohesionless soil occurs, as quoted by Seed and Lee³¹, was the 'critical void ratio' approach suggested by Arthur Casagrande. It was noted that during shear, dense sands tend to expand where as loose sands tend to decrease in volume; thus, for any sand there will be some initial void ratio, termed the 'critical void ratio', for which no volume change during drained shear, (correspondingly, no pore-water pressure changes during undrained shear), will occur. It was reasoned, therefore, that the sand deposits having a void ratio above the critical value and therefore tending to contact during shear, would, under undrained conditions develop positive pore-water pressures that would possibly become large enough to produce liquefaction. Conversely,

deposits having an initial void ratio below the critical value would tend to dilate during shear, producing a decrease in pore-water pressures and a corresponding increase in effective stress, under undrained conditions, so that high strength and stability would be developed.

2.2. Qualitative Approach:

2.2.1 Tests with dry Soil:

Barkan¹ has carried out tests with dry sands and obtained a relationship between the acceleration of vibration and the coefficient of vibro-viscosity assuming the sand to behave like viscous fluid. He assumed the time versus sinking of a sphere to be linear and using Stokes law for static fluid he found out the coefficient of vibro-viscosity. Limitations of his studies will be discussed in the Article 2.4.

2.2.2. Tests with Saturated Soil:

Barkan¹ also conducted tests with different moisture contents in sandy soils. He states, "The forces in Cohesion in soils depends on their moisture content which makes possible to assume that the coefficient of vibro-viscosity also depends on moisture content".

Maslov¹⁹ gave the theory of 'filtration', according to which every sand can be subjected to consolidation under sufficiently intense vibrations. The intensity of vibration depends upon the state of compaction of sand. The compression of sand leads to considerable increase in pore-water pressure.

The sand grains may be looked upon as if they have lost their weight. Thus, depending upon the initial density of sand, there is a 'critical - acceleration' value beyond which there will be an increase in pore-water pressure and decrease in strength and further consolidation of the soil.

Seed and Lundgren³⁰ could not liquefy a loose sand sample with transient loading, at a strain rate of 40 inches per second, although an appreciable decrease in strength was observed in this strain range. They observed "Deformation of a dense sand causes an increase in volume, termed dilatancy, and deformation of a loose sand causes a decrease in volume. Thus if a loose saturated sand is rapidly deformed, the grains tend to move into a more compact condition, and for this to occur, water must flow from the voids. If there is no time for drainage to occur any load on the soil must be carried instantaneously by the pore water, hence, the pressure between the grains is considerably reduced, with a corresponding reduction in the shear strength of the soil. If the strength is reduced to zero, the sand is said to liquefy. On the other hand, when a dense saturated sand is deformed, the void ratio is increased, and if there is no time for seepage into the sand, the water can no longer fill the voids. As a result the pore-water is put into tension (some times called negative pore-water pressure), thereby increasing the pressure between grains and causing a temporary increase in strength".

Matsuo and Ohara²⁰ reported results of tests on loose saturated sands performed on a vibration table. They found a sudden increase in pore-water pressure occurred at a definite acceleration. They confirmed the concept of 'critical acceleration' given by Maslov.¹⁹

Florin and Ivanov¹¹ reported their vibration tests on a 20 cms thick sand deposit, both under steady state and transient vibration. They noted:

- i) If the sand is subjected to shock loading, the whole stratum get liquefied at the same time, while under steady state vibrations the liquefaction starts from the top and proceeds downwards.
- ii) The grain size and superimposed load affect the time for which sand remains in liquefied state.
- iii) Presence of surcharge on the surface of the sands affected the mechanism of liquefaction.

The above mentioned points were also raised by Yoshimi^{38,39}.

Huang-Wen-Xi¹³ obtained test data from triaxial tests performed by Shaking the sample on a vertically vibrating table. He used, density of sand sample, acceleration of vibration and lateral pressure as variables in his study. He showed that the magnitude of pore-pressures depend not only on the physical properties of sand but also on the vibration characteristics.

The phenomenon of liquefaction, he concludes, occurs due to loss of contact between the Grains by dynamic action, there by causing gradual transfer of shear stress from grain to pore-water.

Prakash and Mathur²⁷ studied the effect of frequency and amplitude of vibration on samples of same cross-sectional area but of different heights. Their results show:

- 1) The pore pressure attains a maximum value prior to resonance. At resonance the pore pressure gets partly dissipated.
- ii) Excess hydrodynamic pressure induced is larger than that is required to cause liquefaction.
- iii) Liquefaction of top layers occur first and subsequently the bottom one.
- iv) Settlement of deposit varies characteristically with acceleration of table.

Seed and Lee³¹ concluded on the basis of their test results that the void ratio of the sand, the confining pressure acting on the sand, the magnitude of the cyclic stress or strain and the number of stress cycles to which the sand was subjected determined the danger of liquefaction of a saturated sand. Their conclusions were:

- 1) Higher the void ratio more easily liquefaction will occur.
- ii) Lower the confining pressure more easily liquefaction will develop.

- 111) Larger the stress or strain, lower the number of cycles require to induce liquefaction.

2.3 Analysis of Vibro-floatation:

2.3.1 Effect of Acceleration on Soil Behaviour:

Barkan¹ made extensive studies and gave an empirical relationship between the coefficient of internal friction of sand and acceleration of vibration. It shows as acceleration increases the internal friction decreases and the decrease is rapid upto an acceleration ratio of 5.5 (Fig.2.6) and the relation is expressed as;

$$\tan \phi = (\tan \phi_{st} - \tan \phi_{\infty}) \text{Exp} (- \beta \eta) + \tan \phi_{\infty}$$

where,

$\tan \phi_{st}$ = Value of the coefficient of internal friction without vibration.

$\tan \phi_{\infty}$ = Limit value of the coefficient of internal friction.

η = Ratio of acceleration of vibration to the acceleration due to gravity.

β = A coefficient that determines the effect of vibration (for dry medium-grained sand, $\beta = 0.23$)

It is to be noted that at liquefaction there should not be any internal friction theoretically, but from the above evidence it will not be zero in any case.

2.3.2. Effect of Frequency and Amplitude on Soil Behavior:

These, too were given by Barkan¹. Fig. 2.1 shows the relation between the coefficient of internal friction, ϕ , and the amplitude of vibration for dry medium grained sand frequency remaining the same. The graphs show that the coefficient of internal friction of sand decreases continuously as the amplitude increases and at very high amplitudes it becomes asymptotic.

The dependence of $\tan \phi$ for same angular frequency is more complicated. As frequency increases upto 180 radians per second, the coefficient slowly decreases; then, as the frequency increases still (from 180 to 250 radians per second), the coefficient of internal friction sharply decreases; and subsequent increase in the value of frequency has almost no influence on the coefficient of internal friction. The trend is shown in Fig. 2.2.

2.3.3. Effect of Moisture Content and Grain Size:

It was shown by Barkan¹ that the coefficient of internal friction decreases with the moisture content, the lowest value occurring at 13 percent of moisture content.

He conducted tests on four varieties of sand under two regimes of vibrations to study the effect of grain size. If the effect of vibration is characterized by δ ,

$$\text{where } \delta = \frac{\tan \phi_{st} - \tan \phi}{\tan \phi_{st}},$$

the relationship is given as shown in Fig. 2.3.

2.3.4. Effect of Acceleration on Vibro-viscosity:

Barkan¹ was the first to study the effect of acceleration on vibro-viscosity. He considered the behaviour of finely grained sand subjected to vibratory loads to behave like a fluid and observed the sinking of a sphere in the vertically oscillating dry sand. He utilized Stokes law, which establishes the dependence of velocity of the motion of a sphere in a static viscous fluid on the resistance acting thereon, the radius of sphere and the coefficient of viscosity of the fluid. He expressed the relationship for a sphere falling under the action of gravity in a stationary viscous fluid as:

$$\mu v = \frac{2}{9} r^2 (\gamma_s - \gamma_f)$$

where, μ = Coefficient of viscosity,

v = Steady velocity of the sphere sinking,

r = Radius of the sphere,

γ_s , γ_f are the unit weights of the sphere and the fluid respectively.

In obtaining μ , Barkan did not consider the vibration of fluid (here soil) at all but later, based on experiments he gave a relation between μ and acceleration of vibration as (Fig. 2.4)

$$\frac{1}{\mu} = a (\eta - \eta_0)$$

where, a = A constant coefficient,

η = Ratio of Acceleration of soil to acceleration due to gravity.

η_0 = The threshold of the vibro-viscous state of soil.

It has been established experimentally that the acceleration of vibration lower than $\eta = 1.5g$, does not, practically, affect the coefficient of vibro-viscosity, where, g is the acceleration due to gravity.

2.3.5. Effect of Acceleration on Porosity of Sand:

Barkan¹ describes this relation-ship for fine to medium grained sand on experimental evidence (Fig. 2.6) as:

$$e = e_{\min} + (e_{\max} - e_{\min}) \text{Exp} [-A(\eta + \eta_0)]$$

where,

e = Void ratio at acceleration ratio, η

e_{\max} = Void ratio at the loosest state of soil

e_{\min} = Minimum limit of void ratio of the soil

A = A value depends on moisture content to a maximum value between 0.82 to 0.88.

2.3.6 Effect of Surcharge and Confining pressure:

Florin and Ivanov¹¹ stated that the saturated soil which was placed at a depth more than 15 metres below the ground surface was hardly liquefied.

Ohsaki, as quoted by Kishida¹⁶, showed in his report on damage to R.C.C. Building in Niigata that the upper surface of the liquefied soil layer in the most severely damaged area is mostly situated at depths less than 8 metre.

Kishida¹⁶ estimated the effective overburden pressure of liquefied soil during Niigata earthquake to be approximately 0.8 kg to 1.8 kg. per squared centimetre. He states that a saturated sandy soil is not likely to liquefy if the value of effective overburden pressure exceeds 2.0 kg/cm^2 . He co-relates the 'N' values of Standard Penetration Test with effective overburden pressure and shows the probability of liquefaction of saturated sand as given in Fig. 2.7.

2.4. General Discussion and Development of the Present Investigation:

It can be noted that the critical void ratio is not constant for a given sand, but it depends on the confining pressure to which the sand is subjected. . . This shows an inadequacy of the critical void ratio concept given by Arthur Casagrande, as brought out in section 2.1.

Seed³⁰ writes, "Because the dilation tendencies are smaller at high confining pressure, the critical void ratio decreases as confining pressure increases. Thus it has some times been concluded that a saturated sand at any given density is potentially less stable under a high confining pressure (producing compression characteristics) than under a low confining pressure (Producing dil^atant characteristics)".

The aforementioned approach, by Arthur Casagrande along with Seed's comment, can provide a valuable guide to the behaviour of saturated sand for which the critical void ratio is established, that is, single application of stresses building up from zero to some maximum value. Casagrande noted, as Seed³⁰ quotes, in presenting the concept of critical void ratio, volume changes under cyclic loading conditions are quite different from those occurring under one dimensional static loading condition, and it could hardly be expected that the critical void ratio concept would be applicable to vibratory loading conditions.

However, Maslov¹⁹, noted the "breakdown of Structures associated with sand where the porosity is below 'critical' and, on the contrary, the irreproachable behavior of many structures with the sand porosity above critical".

The aforementioned inadequacies lead the several engineers like, Prakash and Mathur²⁷, Maslov¹⁹ etc. to attempt to establish the conditions producing liquefaction in terms of acceleration at which the phenomenon can be observed to develop.

The limitations of Barkan's study as shown in sections 2.2.1 and 2.3.4, is due to the fact that he did not consider the vibration of the soil in determining the coefficient of vibro-viscosity and at the same time he assumed sinking of the sphere with time to be linear, which is not true as it is evident from his experimental curves.

It is, therefore, proposed to consider the vibrating soil as vibrating viscous fluid and then find out a solution for the sphere in an oscillating fluid under the action of gravity.

2.5 Accelerated Motion of Sphere in a Fluid:

Stokes investigated the simple harmonic and rectilinear oscillations of a sphere, a cylinder and an infinitely long flat plate in a viscous fluid. He omitted the convective acceleration terms in the Navier-Stokes equation and derived the expressions for forces exerted by the fluid on these objects. Each expression consists of two terms, one involving the acceleration and the other the velocity and both includes viscosity.

Later Basset^{2,3}, Boussinesq and Oseen¹⁷ studied the rectilinear motion of a sphere which has a rapid but arbitrary acceleration in a viscous fluid. They also omitted convective acceleration terms in the Navier - Stokes equation in deriving their equation of motion. They postulated that the force on the sphere depends not only on its instantaneous velocity and acceleration but also, on a term, which will be termed as Basset's 'History Integral', which represents the effect of its entire history of acceleration. Each effect is represented by a separate term. It is also important to note that the acceleration term does not include viscosity.

In fact, this term is the same as the expression derived for an inviscid and irrotational flow.

Basset^{2,3} presented the equation of motion (accelerated) of a sphere falling in a viscous fluid under the influence of gravity in which the resistance is a linear function of velocity. He also assumed that for slow motions (as is the case here) the squares and the products of velocities can be neglected. Thus the equation of Basset reads;

$$(m_s + km_f) \frac{dv_s}{dt} + 3\pi\mu d v_s + \frac{3}{2} d^2 \sqrt{\pi\mu\rho_f} \int_0^t \frac{\frac{d}{d\tau}(v_s) d\tau}{(t-\tau)^{3/2}} = (m_s - m_f) g \quad \dots (2.4)$$

where

- m_s = Mass of the sphere
- m_f = Mass of the fluid displaced by sphere
- k = Added mass coefficient (= 1/2 for sphere)
- v_s = Velocity of the sphere
- d = Diameter of the sphere
- ρ_f = Density of the fluid
- τ , is any time, $0 \leq \tau \leq t$
- μ = Coefficient of viscosity of the fluid
- g = Acceleration due to gravity.

The solution for equation 2.1, is given by several persons like Basset^{2,3}, Lamb¹⁷, Brush et al⁶, Hjelmfelt et al²², Lord Rayleigh²⁹ etc., but each solution has got

limitation one or other and also they can not be applied to the case of an oscillating fluid.

Based on these concepts, a detail out line of the solution for the accelerating motion of a sphere in an oscillating fluid will be presented in the next chapter.

CHAPTER - III

3.1 Introduction:

It has been established in Chapter II, that the soil, subjected to intense vibrations or shock loads, tends to behave like a fluid. In order to study the behavior of structures on such a soil, some of the parameters, like the vibroviscosity of the soil etc. have to be analysed. With that in view, the classic problem of the accelerated motion of a sphere in vibrating soil continuum has been analytically studied in this chapter, idealizing the soil medium to behave like an oscillating fluid. Numerical solutions have been attempted for the resulting equation of motion and results are graphically shown.

The basic study of the accelerated motion of a sphere in an oscillating-fluid was due to Carstens⁸ who obtained the solutions making several simplifying assumptions. In this study the basic equations have been modified in the light of the analysis presented in sec. 2.5, to suit the problem under consideration.

3.2 Accelerated motion of a Sphere in an Oscillating fluid:

It will be assumed that the sphere is falling under the action of gravity. An one-degree of freedom system will be assumed throughout the analysis and it is also assumed here that the fluid is oscillating with Simple Harmonic Motion.

Now let,

a = Position co-ordinate of the fluid,

\dot{a} = Velocity co-ordinate of the fluid,

\ddot{a} = Acceleration co-ordinate of the fluid;

x = Position co-ordinate of the sphere,

\dot{x} = Velocity co-ordinate of the sphere,

\ddot{x} = Acceleration co-ordinate of the sphere;

m_s = Mass of the sphere,

ρ_s = Mass density of the sphere,

m_f = Mass of the volume of fluid displaced by the sphere,

ρ_f = Mass density of the fluid,

μ, ν = Coefficient of vibro-viscosity and Kinematic viscosity of the fluid, respectively.

k = Added mass coefficient of the sphere
= 1/2 for sphere.

d = Diameter of the sphere.

The forces involved in this type of motion are as follows:

$m_s \ddot{x}$ = Inertial reaction of the sphere,

$m_f \ddot{a}$ = Force exerted by the fluid on every fluid volume,

$k m_f (\ddot{a} - \ddot{x})$ = Virtual mass effective force.

Dissipative forces on the sphere

$$= 3\pi\mu d(\dot{a} - \dot{x}) + \frac{3}{2} d^2 \sqrt{\pi \rho_f \mu} \int_0^t \frac{\frac{d^2}{d\tau^2} (a-x) d\tau}{\sqrt{t-\tau}}$$

This is directly from Eq. 2.1.

On account of the pressure gradient in the fluid, if the fluid is accelerated in the direction a , there is a force $(m_f \ddot{a})$ on the sphere. The force $km_f(\ddot{a}-\ddot{x})$ is the virtual mass multiplied by the relative acceleration between the fluid and sphere. This simple treatment is possible in a system with one-degree-of-freedom, since the acceleration is a true vector in this co-ordinate system.

The History Integral:

This term is a type of history term which indicates that the resistance to motion at any time t , due to unsteadiness of the flow, is, in part, a function of the resistance at a previous time. This corrects for the transient character of the velocity distribution. The derivation of the appropriate History Integral for the oscillating fluid has been derived in Appendix -II.

Thus using Newton's law, the equation of accelerated motion of a sphere in an oscillating fluid can be written as;

$$m_s \ddot{x} = m_f \ddot{a} + km_f (\ddot{a}-\ddot{x}) + (m_s - m_f) g + 3\pi\mu d (\dot{a}-\dot{x}) + \frac{3}{2} d^2 \sqrt{\pi \rho_f \mu} \int_0^t \frac{\frac{d^2}{d\tau^2} (a-x) d\tau}{\sqrt{t-\tau}} \quad \dots (3.1)$$

Assuming the fluid motion as;

$$a = a_0 \sin \omega t \quad \dots (3.2)$$

where, a_0 = Half amplitude of fluid motion, and
 w = Angular velocity of fluid motion.

The Eq. 3.1 takes the form;

$$\ddot{x} + \frac{18 \gamma}{\left(\frac{\rho_s}{\rho_f} + k\right) d^2} \dot{x} + 9 \frac{\sqrt{\gamma/\pi}}{\left(\frac{\rho_s}{\rho_f} + k\right) d} \int_0^t \frac{\frac{d}{d\tau} \left(\frac{dx}{d\tau} - w a_0 \cos w\tau \right) d\tau}{\sqrt{t - \tau}} d\tau$$

$$= -w^2 a_0 \frac{(1+k)}{\left(\frac{\rho_s}{\rho_f} + k\right)} \sin w t + \frac{\left(\frac{\rho_s}{\rho_f} - 1\right)}{\left(\frac{\rho_s}{\rho_f} + k\right)} g$$

$$+ \frac{18 \gamma}{\left(\frac{\rho_s}{\rho_f} + k\right) d^2} w a_0 \cos w t \quad \dots (3.2)$$

Non-dimensional form:

Eq. 3.3 can be written in the non-dimensional form,
 using;

$$X = \frac{x}{L} \implies x = XL$$

$$T = \frac{\gamma t}{d^2} \implies t = T \frac{d^2}{\gamma}$$

where, L = Any characteristic length; Here the depth of
 fluid upto which the readings can be taken.

Thus:

$$\frac{dx}{dt} = \frac{\gamma L}{d^2} \frac{dX}{dT}; \quad \frac{d^2 x}{dt^2} = \frac{\gamma^2 L}{d^4} \frac{d^2 X}{dT^2}$$

Again, let, $\frac{\rho_s}{\rho_f} = R$, the density ratio of sphere to fluid,

$$\text{and } RA = \frac{a_0}{L}, \quad RB = g/w^2 L$$

N_s = A number equivalent to Stokes number

$$= \sqrt{\frac{\gamma}{w d^2}}$$

So then, the non-dimensional form of the Eq. 3.3, reduces to;

$$\begin{aligned} \frac{d^2 X}{dT^2} + \frac{18}{(R+k)} \frac{dX}{dT} + \frac{1+k}{(R+k)} \frac{RA}{N_s^4} \sin(T/N_s^2) - \frac{18}{(R+k)} \frac{RA}{N_s^2} \\ \cos(T/N_s^2) - \frac{(R-1)}{(R+k)} \frac{RB}{N_s^4} \\ = - \frac{9 \sqrt{\gamma/\pi d^2}}{(R+k)} \times \frac{d^4}{\gamma^2 L} \int_0^t \frac{\frac{d}{d\tau} \left(\frac{dx}{d\tau} - w a_0 \cos w \right) d\tau}{\sqrt{t-\tau}} \end{aligned}$$

... (3.4)

Multiplying each side by $(t-\tau)^{1/2}$ and integrating with respect to τ ^{6,29}, denoting the left hand side as $F(T)$;

$$\int_0^t \frac{F(T)}{\sqrt{t-\tau}} d\tau = - \frac{9 \sqrt{\gamma/\pi d^2}}{(R+k)} \frac{d^4}{\gamma^2 L} \int_0^t \frac{d\tau}{\sqrt{t-\tau}} \int_0^t \frac{\frac{d}{d\tau} \left(\frac{dx}{d\tau} - w a_0 \cos w \tau \right)}{\sqrt{t-\tau}} d\tau$$

... (3.5)

$$\text{Let } G(t) = \int_0^t \frac{d}{d\tau} \left(\frac{dx}{d\tau} - w a_0 \cos w \tau \right) \frac{d\tau}{\sqrt{t-\tau}} = \int_0^t \frac{F'(\tau) d\tau}{\sqrt{t-\tau}}$$

Then the double integral,

$$\int_0^t \frac{G(\tau) d\tau}{\sqrt{t-\tau}}, \text{ using 'Abel's' theorem;}$$

$$= \pi [F(t) - F(0)]$$

Thus Eq. 3.4 yields,

$$\int_0^t \frac{F(\tau) d\tau}{\sqrt{t-\tau}} = \frac{-9 \sqrt{\gamma/\pi} d^2}{(R+k)} \frac{d^4}{\gamma^2 L} \pi \left(\frac{dx}{dt} - w a_0 \cos wt \right)$$

Using $(\dot{x} - \dot{a}) \Big|_{t=0} = 0$

Thus the non-dimensional form of Eq. 3.1 reduces to;

$$\frac{d^2 X}{dT^2} + P \frac{dX}{dT} + \frac{.442 P}{\sqrt{T}} \frac{dX}{dT} + Q \sin(T/N_s^2) - S \cos(T/N_s^2)$$

$$- M - \frac{N}{\sqrt{T}} (\cos(T/N_s^2) - 1) = 0 \quad \dots (3.6)$$

Where, $P = 18/(R+k)$ $S = P \cdot RA/N_s^2$

$$Q = \frac{1+k}{R+k} \cdot RA/N_s^4 \quad M = \frac{R-1}{R+k} \cdot \frac{RB}{N_s^4}$$

$$N = .442 P \cdot RA/N_s^2$$

The Eq. 3.6 is the final equation governing the accelerated motion of a sphere in an oscillating fluid in the dimensionless form.

3.3 Numerical Solution for the Governing Equation:

A fourth order Runge-Kutta method will be used for solving the Eq. (3.6).

The equation is broken up into two first order simultaneous differential equations as follows,

$$\frac{dX}{dT} = Z \quad \dots (3.7a)$$

$$\begin{aligned} \frac{dZ}{dT} = & S * \cos(T/N_s^2) + M + \frac{N}{\sqrt{T}} (\cos(T/N_s^2) - 1) \\ & - P (1 + .442/\sqrt{T}) * Z - Q * \sin(T/N_s^2) \end{aligned} \quad \dots (3.7b)$$

Thus, there are two dependent variables X and Z and one independent variable T.

Difficulty with the Eq. (3.7) is, although,

$$\left. \frac{dX}{dT} \right|_{T=0} = RA/N_s^2 \text{ and } \left. X \right|_{T=0} = 0,$$

but $\frac{d^2X}{dT^2} = \frac{dZ}{dT} \Big|_{T=0}$, can not be evaluated directly

and only a limiting value is possible at $T = 0$, owing to its singularity at $T = 0$.

However, the limiting value of $\frac{dZ}{dT}$ as $T \rightarrow 0$ can be found

as, $\frac{dZ}{dT} = M$, when T is very close to zero.

Upto a certain range of T the value of X and Z will be obtained from the limiting value of $\frac{dZ}{dT}$ and after that, the calculation will be carried out using Eq. (3.7b). The validity of such an approximation is verified in the sec. 3.6.

3.4 Runge-Kutta Method with Gill's Variation:

This method comes under the general category of Runge-Kutta methods and is a modified version of Runge-Kutta fourth order method. The derivation of this method can be found in many text books on numerical analysis²⁸.

The Runge-Kutta numerical integration method is a non-iterative, step by step and self starting procedure. This method is suitable here as the problem dealt here is an initial value problem having two boundary conditions at the starting point of the integration. Accuracy of this method is derived by using several estimates of the dependent variable for each increment of the independent variable. Usually the method is set up for first order equations. However, it can be easily adopted to higher order equations. A second order differential equation, as in this case, is handled by first transforming them into a set of first order differential equations (Eq.3.7).

The truncation error for one integration step is of order $(dT)^5$ for this fourth order method, where (dT) is the

increment of independent variable. Theoretically, there are no limits on the increment size in regard to convergence and stability. The size of the time increment of integration is decided so that it is not too small as to require excessive computation labour or result in large round off error; neither it should be so large as to give rise to large truncation errors (the variation with respect to step size is shown in Fig. 3.2)

When the time increment of integration is increased less computer time is needed for the solution of a given problem, but beyond a certain limit of increment the solution obtained would deviate more and more from the true solution, and instability in the numerical integration is said to have occurred and so there is a limit as to the larger time increment that can be used in the integration. The increment (ΔT) is 0.05 as is taken here.

3.5 Comparison of the Solutions Obtained with the Existing Results:

3.5.1 Carstens's⁸ Solution:

This solution is essentially the same equation as 3.1, neglecting the history integral of Basset. The non-dimensional form of the equation is thus;

$$\frac{d^2x}{dT^2} = S^* \cos(T/N_s^2) - P \frac{dx}{dT} - Q \sin(T/N_s^2) + M \quad \dots (3.8)$$

Results of the equation (3.8) are shown in Figs. 3.1 to 3.4 and discussed in the article 3.6.

3.5.2 Wagenschein's Solution:

As quoted by Carstens⁸ Wagenschein conducted some experiment on the oscillating motion of sphere in an oscillating fluid. Carstens checked these results using viscous drag and Added mass coefficients given by Stokes, using Lamb's¹⁷ solution.

The maximum displacement of the half amplitude of fluid motion to sphere motion in an oscillating fluid given by König (quoted by Carstens) is as follows;

$$\frac{x_o}{a_o} = \sqrt{\frac{(1+k)^2 + (A/m_f w)^2}{(R+k)^2 + (A/m_f w)^2}} \quad \dots (3.9)$$

where, x_0 = Half amplitude of sphere motion and fluid motion
is, $a = a_0 \sin \omega t$, same as shown in equation (3.1).

To apply this to the case of oscillating sphere, the coefficients A and k have to be changed to:

$$\text{Viscous drag coefficient, } A = 3\pi\mu d \left(\frac{1+N}{N} \right) \quad \dots (3.10)$$

$$k = \frac{1}{2} + \frac{9}{4} N$$

$$\text{where, } N = \frac{1}{d} \sqrt{\frac{8\gamma}{w}}$$

For such a case the equation (3.5) reduces to:

$$\begin{aligned} X = P * (1. + .442/\sqrt{T}) * ((8/N_s^2) * \cos(8T/N_s^2) - \dot{X}) \\ - \frac{(1+k)}{(R+k)} * (64/N_s^4) * \sin(8T/N_s^2) \quad \dots (3.11) \end{aligned}$$

Where $X = x/a_0$, a_0 = half amplitude of fluid motion

$$P = 18/(R+k)$$

$$N_s = \sqrt{\frac{8\gamma}{wd^2}}$$

These results are compared using, $A = 1.0$ and k , the added mass coefficient to be equal to half. They were plotted in Fig. 3.14 and are discussed in the article 3.6.

3.6 Discussion:

To start with the solution of Eq. (3.6), the applicability of the Runge-Kutta integration technique to the present problem is justified by comparing the numerical solution of the static case of Eq. (3.1), with the existing solutions. One such solution is reported by Hjelmfelt et al¹² and his solution is verified using the following computations; Eq. (2.1), can be rewritten as;

$$\begin{aligned} \pi \frac{d^3}{6} (\rho_s + k \rho_f) \frac{dv}{dt} &= (\rho_s - \rho_f) g \frac{\pi d^3}{6} - 3\pi \mu_f v d \\ &\quad - \frac{3}{2} d^2 \rho_f \sqrt{\pi g} \int_0^t \frac{\frac{dv}{d\tau} d\tau}{\sqrt{t-\tau}} \end{aligned} \quad \dots (3.12)$$

which ultimately converts (Using Abel's Transformation) to:

$$A \frac{dv}{dT} + (1 + 4.43/\sqrt{T}) V = 1 \quad \dots (3.13)$$

where, $A = (R + k)/18$, $R = \text{Density ratio}$

$V_t = \text{Stokes terminal velocity or terminal Reynold's number} = (R-1) g d^3 / 18 \nu^2$

$T = \text{Time factor} = \nu t / d^2$

$V = \left(\frac{d}{4}\right) \frac{v}{V_t}$, where v is the velocity of sphere.

The solutions of the eq. (3.13) are shown in the Figs. 3.12 and 3.13, they show an excellent agreement with the existing solution given by Hjelmfelt et al¹².

The figures 3.1 to 3.11 show the solutions of the Eq. (3.6), depending upon the various magnitudes of non-dimensional variables namely, N_s , RA , RB and R . In most of the cases Carstens's⁸ solutions are also presented and it has to be born in mind that the solutions reported by Carstens⁸ are essentially the solution of the Eq. 3.6 neglecting Basset's history integral. It is worth mentioning that Carstens's solution gives much higher values of displacement (as high as 20%) than the actual solution (Eq. 3.6).

To read the graphs the following notations are followed:

In Fig. 3.1: A, denotes the proposed solution of the Eq. (3.6),

B, denotes Carstens's solution, and the density ratios are shown in the bracket.

Here, B(5.0) denotes, the Carstens's solution with density ratio, $R = 5.0$, and same is the case for A(5.0), which denotes, the proposed solution with $R = 5.0$.

In almost all the results two variables were kept constant while the other two were varied. In Fig. 3.3, A(5.0)3 denotes a true solution with the density ratio, $R = 5.0$ and keeping RA and RB constant, the magnitude of the other variable is 0.1, which is the case 3 of N_s variation. This procedure is followed throughout the representation of the solution.

As N_s increases, it can be observed that the deviation of the Carstens's solution from the true solution is more.

The solutions are given in terms of displacement - time relationship, keeping the practical utility of these solutions in view.

In Fig. 3.3, it is observed that the time-displacement relationship is a linear after a certain time interval, which indicates a little change in the nature of solutions with the change of kinematic viscosity.

It can be seen from the Fig. 3.4 that as the amplitude of vibration varies, the nature of solution also changes. As an example, for $RA = 0.01$, after a certain time the magnitude of velocity decreases and then becomes steady, whereas for the other values of RA , the variation of velocity is of increasing order and then becomes steady. In lower density ratios, of course, the nature of variation is nearly same as for higher RA values. Thus, it can be concluded that at lower density ratios the role of amplitude variation is appreciable. This can be noticed also from Figs. 3.6 and 3.8.

Except for lower density ratios, the role of acceleration ratio, RB , is not predominant. This can be observed in the Figs. 3.5, 3.7 and 3.9.

It can be noticed from the Figures 3.10 and 3.11 that at the higher values of the variables (N_S , RA , RB), the time - displacement relation is almost linear.

The Fig. 3.14, gives a comparative study of the presented solution with that of König's results. It is to be

noted that for higher density ratios, two solutions converge. Again, it is worth mentioning that at lower values of N_S , the variation is appreciable, again at higher values of N_S (i.e. of $\dot{\gamma}$ or lower values of w) the proposed solution deviates appreciably from König's solution. Although, König's solutions are experimentally verified by Carstens³, Wagenschein⁸, still, they are approximate solutions of Eq. 3.6 neglecting history term of Basset.

CHAPTER - IV

EXPERIMENTAL SET UP

4.1 Objective:

The present laboratory investigation was carried out with the following objective;

To evaluate the vibro-viscosity, μ , using conventional method and its variation with respect to frequency, load and Grain Size characteristics of the soil, and then compared with the solutions presented in the previous chapters.

4.2 Instrumentation:

Small scale vibratory tests usually employ mechanical oscillators which generate sinusoidal forcing function. Though the generation of sinusoidal forcing function is not an absolute necessity, analyses of the data become extremely complicated with any other type of forcing functions. Again, any type of function, used in the analysis, may be transformed into an equivalent sinusoidal function.

In the present investigation an electrically operated oscillator, under the trade name "Unholtz-Dickie"* Shaker was used.

* Vibrating testing System No. 72

Shaker: Model No. 105, by Unholtz-Dickie Corporation.

Capacity: Generated force: 180 lbs. peak

Maximum free table acceleration: 42 g.

Shaker Stroke: 1 inch

Free table resonant frequency: 5000 cps.

The test equipment available here includes three separate vibration Test Systems. Each system is rated at 180 lbs of generated force. Usable frequency range is 5 cps to 100 kcs. Each system can be operated independently of the systems can be driven from a common oscillator.

4.2.1 Simultaneous Operation of Three Systems:

In the system of operation as shown in Fig. 4.1, the console containing the BK 1039 Servo-oscillator is known as the master console. The two consoles without oscillators are slave consoles. In this mode of operation all Shakers are driven simultaneously at the same frequency. The BK 1039 servo-oscillator maintains the acceleration or displacement level at one point constant.

The arrangement, shown in Fig. 4.1, will increase or decrease the vibration level of each shaker simultaneously by an equal amount, if the vibration level of each shaker varies. Each shaker is equipped with its own BK 1039 servo-oscillator. In this case the 1039's are interconnected in such a manner that the oscillator section of the 'Master' 1039 drives all the shakers, but the servo-oscillator section in each 'slave' 1039 maintains the acceleration level at the corresponding shaker at the desired level.

4.2.2. Single Operation:

Each system can be operated independently. The slave console requires an oscillator signal input.

The operation employed here is, the master is directly attached to one of the three shakers and acceleration level is made constant, with varying frequency from 25 cps to 250 cps.

4.2.3 Description of System:

The vibration system consists of three parts, the shaker, the control console, and the Electronic Power Amplifier.

4.2.3a Shaker:

The shaker is the important part of the system. It provides the vibrating table to which the items to be tested are attached. The principal parts of the shaker is shown in the Fig. 4.2.

The water cooled field coils energize the shaker body with flux paths as shown creating a high magnetic flux density in the annular air gap. The field coils are connected to a d-c power source. The armature assembly, consisting of the table and the driver coil, is suspended from the shaker body by the Unholtz-Dickie table suspension. When an alternating current is passed through the driver coil, an electro dynamic force is generated in the driver coil wires causing the table to move as indicated by the double ended arrow drawn on the table. The frequency of the alternating current determines the frequency of vibration in the table. The motion of the table is limited by the maximum stroke of the shaker, available voltage from the electronic power amplifier in the low

frequencies and by the rated force or maximum acceleration in the higher frequencies. The shaker is trunion mounted allowing it to be oriented for vertical or horizontal vibration or any position between the limits. The operation employed here only the horizontal position of the shaker is utilized.

4.2.3b Electronic Power Amplifier:

The electronic Power Amplifier input is connected to the controlling oscillator signal source and the out put is connected to the driver coil of the shaker. The oscillator generates a low power, low voltage signal which is amplified by the Electronic Power Amplifier to the necessary power and voltage levels to cause the alternating currents to flow through the driver coil as required to generate rated force. The Amplifier is of straight forward design to provide the necessary power levels through the operating frequency range without introduction of significant distortion.

4.2.3c Control Console:

The control console contains the Automatic Shaker Control, the Adjustable Power supply for the shaker field, the Dial-A-Gain and the control circuitry, pilot-lights, driver coil and field coil ammeters, interlocks and the system 'on-off' switch.

The Automatic shaker control consists of the Oscillator, the Automatic Level control and the Vibration Meter.

The oscillator originates the signal voltage which is fed to the Power Amplifier, which in turn causes an alternating current to pass through the driver coil of the shaker. The driver coil current causes the shaker table motion. Thus the frequency and magnitude of shaker table motion is controlled by the frequency and voltage generated by the oscillator.

The automatic level control adjusts the magnitude of the oscillator output voltage fed to the power amplifier to account for variations in system frequency response due to resonant characteristics of the items mounted on the shaker table and the inherent shaker system response itself.

In the case here, the frequency is varied manually while the automatic level control maintains the set value of acceleration.

The adjustable field supply is provided to give more flexibility in system operation. If full rated generated force is not required for a particular test, the operator may reduce the field current in order to minimize the already low magnetic leakage flux at the table surface or increase the obtainable low frequency table displacement.

The Dial-A-Gain is a multipurpose instrument which allows monitoring acceleration from any piezo electric accelerometer. It includes a high impedance cathode follower input and a variable gain amplifier.

4.3 Testing Procedure:

For the present test program, an aluminium tank of 29.8 by 29.8 cms in cross section and 49.6 cms high is filled with sand (Grain size analysis of the sand is shown in Fig.(5.12)). The tank is mounted on the base plate (50 cm x 50 cms) which in turn is fixed rigidly to the shaker table (Fig. 4.3). This shaker table can be subjected to vertical vibrations of a selected amplitude and frequency.

A mild steel frame is fabricated from which a metallic (brass) sphere of 2 cm dia. is placed on the soil surface. A load is imposed on this sphere by means of a thin brass (3 mm dia) rod. There is one counter weight which is **suspended** from a friction-less pulley by a non extensible silk thread. The other end of the thread goes to the small platform, through another pulley, from which the load is imposed on the sphere. The counter weight slides over a smooth square section rod which is graduated. The combination of the rod and the counter weight makes a vernier arrangement, as result, it is possible to measure the displacement of the counter weight upto 0.001 ft. (The arrangement is shown in Fig. 4.3).

Before running the each test, the sand is compacted by vibrating the soil. The frequency level is increased gradually keeping the acceleration level constant. The sinking of the sphere at different loading condition and frequency is noted by noting the displacement of the counter weight.

For each set of run the acceleration level is kept constant at 1.0g and the frequency is varied from 25 cps to 250 cps.

Using Visicorder the vibration characteristics of sand is recorded and typical responses are shown in Figs 5.16 to 5.19

The experiment carried out with the soils of different Grain sizes (Fig. 5.12).

TEST RESULTS5.1 Test Data:

The experiment was conducted at frequencies ranging from 25 cps to 250 cps. At each frequencies for different loading conditions from the upper disc of the loading platform, the sinking of sphere is noted from the vernier scale arrangement. The loading conditions are ranging from 1 lbs to $2\frac{1}{2}$ lbs from the top. The sinking of sphere versus time relations are shown in the figures 5.1 to 5.4 and then 5.8 to 5.11.

The displacement-time and acceleration-time responses are noted by Visicorder and are shown in figures 5.16 to 5.19

The experiment is carried over on two soil samples (Fig. 5.12).

5.2 Soil Behavior:

The soil medium chosen is medium fine dry sand. The physical properties of the soil are:

Sample I:

Specific gravity, $G_s = 2.50$

Minimum void ratio, $e = .468$

Bulk density, $\gamma_s = 1.74 \times 10^3 \text{ kg/m}^3 = 109 \text{ pcf.}$

Sample II:

Specific gravity, $G_s = 2.55$

Minimum void ratio, $e = .412$

Bulk density, $\gamma_s = 1.81 \times 10^3 \text{ kg/m}^3 = 113 \text{ pcf.}$

The Grain size distributions are shown in the Fig. 5.12. To obtain minimum void ratio the sand is vibrated for one minute at each frequency from 25 to 250 cps and after such an operation the void ratio is calculated (Before vibration the void ratios were, .724 and .546, respectively). According to M.I.T. classification the sand for the first set is a medium sand and the second set falls under coarse sand group.

5.3 Vibro-viscosity:

The experiment shows that when the sand sample is subjected to intense vibration the forces of internal dry friction between the particles vanish and assume the mechanical properties of a viscous fluid. Thus the solid bodies placed on this sand will sink into it with a certain velocity if their densities exceed the density of the sand. This mechanical property is designated by the coefficient of vibro-viscosity.

The main object of the experiments carried out so far is to determine this coefficient and apply this information to the sinking behavior of piles due to liquefaction. First of all the viscosity will be determined using Stokes classical method where by neglecting any effect of vibration of sand and neglecting the inertia and history integral of the Eq. (2.1). And then the actual solution for an oscillating fluid will be brought in to justify the first one.

5.3.1 Stokes Solution:

If a spherical body descends through a semi-infinite viscous fluid with constant velocity V , Stokes law says,

the viscous drag, $3\pi\mu dV$, is equal to the buoyant force $(m_s - m_f)g$. The terms have already been explained in the Chapter III.

Thus, Downward force = buoyancy + resisting force

$$\text{That is, } F + \frac{\pi}{6} d^3 \rho_s g = \frac{\pi}{6} d^3 \rho_f g + 3\pi\mu d,$$

$$3\pi\mu dV = \frac{\pi}{6} d^3 (\rho_s - \rho_f) g + F \quad \dots (5.1)$$

Now, in addition to this it will be assumed that the load on the upper disc will only increase the density of the sphere in the following way;

Let, F be the load acting on the sphere in addition to its own weight, then if γ_E be the equivalent increase of unit weight then,

$$\gamma'_E = \frac{6F}{\pi d^3} \quad \dots (5.2)$$

and actual γ_s will be,

$$\gamma_s = \gamma'_s + \gamma_E \quad \dots (5.3)$$

where, γ'_s is the unit weight of sphere material.

Now, from equation (5.1)

$$\mu = \frac{d^2 (\dot{\gamma}_s - \dot{\gamma}_f)}{18 V} \quad \dots (5.4)$$

Using equation (5.4) and utilizing the velocities for different cases as noted in the Fig. 5.1 etc the vibro-viscosity versus frequency relations are obtained (Figs. 5.12 & 5.13).

To obtain a representative value of the Kinematic viscosity, $\dot{\gamma}$, the following deductions were used:

Obtained μ in Eq. (5.4) is in the unit gmf - sec/cm².
To convert this into lbf - sec/ft²,

$$1 \frac{\text{gmf} - \text{sec}}{\text{cm}^2} = .205 \text{ sec} - \text{lbf/ft}^2 \quad \dots (5.5)$$

. Now to get density of the sand, if, Sp. gr. = G_s ,

$$\text{density} = 1.94 G_s \text{ Slug/ft}^3$$

Thus Kinematic Viscosity of sand, using Eq. 5.4, is

$$\dot{\gamma} = \frac{\mu}{G_s} \times .107, \text{ ft}^2/\text{sec.} \quad \dots (5.6)$$

The values of $\dot{\gamma}$ with various frequencies are given in the Table 5.1.

5.3.2 Verification of Experimental results:

To verify the results obtained in the previous section with the solution proposed in the Chapter III, the following computations are made;

The Eq. (3.1) can be rewritten in the form:

$$\ddot{x} = P_2, \quad A_2 + P_M + P_1 \cdot A_1 - P_1 \cdot \dot{x} \quad \dots (5.7)$$

in which,

ν = Kinematic viscosity of fluid, d = diameter of the sphere

R = Density ratio; k = Added mass coefficient

$$P = 18/(R+k), \quad Q = 7.98 \sqrt{\nu/d^2}$$

$$P_1 = P \cdot \sqrt{\nu/d^2} + Q/\sqrt{t} \quad P_2 = \frac{1+k}{R+k}$$

$$A_1 = w a_0 \cos wt \quad A_2 = w^2 a_0 \sin wt$$

$$P_M = ((R-1)/(R+k))g; \quad g = \text{acceleration due to gravity}$$

Notations are similar as they were described in the Section 3.2.

Eq. 5.7 is evaluated using the same numerical integration technique, using, ν as variable for different set of results. An approximate value of ν can be obtained from equation 5.6. Now, as the variables R , d , w , g , a_0 are known before hand, the only variable remains to be determined is ν . Taking neighbouring values of ν , as it is obtained from Eq. 5.6, the variation of the results are reported by varying the values

of γ . The results are shown, along with the experimental data, in the Figs. 5.14 and 5.15.

To illustrate the utility of the proposed solution (Eq. 3.1), one set of test results are considered and compared with the solution of Eq. 5.7, with,

Applied load, $F = 2.5$ lbs

Frequency, $f = 200$ cps

So. Gravity, $G_s = 2.5$, and with other

variables remaining constant. These results are plotted in the Fig. 5.14. It can be observed from the Fig. that the Kinematic viscosity, γ , as obtained from this analysis is much lower than the one calculated from Stokes solution (Eq. 5.6). For example, from the Fig. 5.14, the Kinematic viscosity range at which the experimental data falls is from 200 to 300 ft^2/sec , although the Kinematic viscosity is equal to 420 ft^2/sec using Stokes solution Eq. (5.6), which is the same as was used by Barkan¹.

The reason for this deviation is due to the fact that, in obtaining γ from Eq. 5.6, the oscillation of the fluid is not taken into account and also the solution is an approximate one using steady velocity of a sphere in a stationary fluid. This argument is applicable, as well, for the other set of experimental values.

It can be noticed from the figures 5.12 and 5.13 that there exists a definite frequency at which Vibr-viscosity is minimum for a particular soil. In the case I, it is 210 cps

and for Case II it's very near to 170 cps.

The main draw back of the experiment is that the wall effect of container is totally ignored, although it may contribute some discrepancy to the results obtained with the theory.

5.4 Visicorder Records:

To evaluate the response in the soil medium a magnetic pick up is fixed on a platform in the soil medium. It is observed in the Figs. 5.16 to 5.19, that the response gives sufficient accurate displacement-time relationship at lower frequencies but as the frequency increases the response nature becomes somewhat erratic. Although the input acceleration in all the cases where g , which were mentioned in the Figs. 5.1 to 5.4 and then in 5.8 to 5.11, but the visicorder records show some deviations. As for example, in the Fig. 5.4, constant acceleration is shown as g but visicorder records (Fig. 5.19) show that the magnitude of acceleration is $0.7g$ instead of g . The calculations were made using the later acceleration, in comparing the laboratory results with the theory.

TABLE 5.1

Sample I : $G_s = 2.5$, $e_{min} = 0.468$, $\gamma_s = 109$ pcf

Load (lbs)	Frequency (cps)	Coefficient of viscosity, μ , (lbf-sec/ft ²) x 10 ⁻⁴	Kinematic viscosity, ν , (ft ² /sec) x 10 ⁻⁴
1.0	25	4.16	0.857
1.0	30	6.23	1.280
1.0	50	3.12	0.640
1.0	100	2.97	0.610
1.0	170	0.69	0.140
1.0	200	0.56	0.117
1.0	230	0.62	0.120
1.0	250	1.25	0.250
1.5	200	1.31	0.270
1.5	230	1.31	0.270
1.5	250	0.51	0.100
2.0	190	3.04	0.620
2.0	200	1.74	0.320
2.0	220	4.05	0.830
2.0	250	3.47	0.710
2.5	190	1.89	0.390
2.5	200	0.20	0.042
2.5	220	1.16	0.230
2.5	250	3.78	0.770

Sample II : $G_s = 2.55$, $e_{min} = 0.412$, $\gamma_s = 113$ pcf.

Load (lb)	Frequency (cps)	Coefficient of viscosity, μ , (lbf-sec/ft ²) $\times 10^{-4}$	Kinematic viscosity, ν , (ft ² /sec) $\times 10^{-4}$
1.0	170	1.04	0.21
1.0	190	1.04	0.21
1.0	200	1.56	0.32
1.0	250	1.56	0.32
1.5	170	1.02	0.21
1.5	190	2.30	0.47
1.5	200	2.30	0.47
2.0	170	2.02	0.41
2.0	190	2.02	0.41
2.0	200	2.43	0.50
2.0	250	4.05	0.83
2.5	190	1.89	0.39
2.5	200	2.04	0.42
2.5	250	2.04	0.42

CHAPTER - VI

GENERAL DISCUSSION AND CONCLUSIONS

Experimental and analytical studies have been conducted in this investigation to study the motion of a sphere in a vibrating soil medium. The vibro-viscosity of the fluidised soil medium has been evaluated for a wide range of frequencies using Stokes solution and some of these values are compared with the modified analysis presented in Chapter III. The effect of grain size frequency, load applied on the sphere etc. on the accelerated motion of the sphere have been studied and are graphically presented. Relevant conclusions have been presented, earlier, for each chapter. General conclusions from this investigation have been listed below:

The experiments conducted, here in, reveal that, even if the ground acceleration is lower than that of the value given by Barkan¹ as threshold acceleration (1.5g) for fine to medium grained dry sand, liquefaction during the process of vibro floatation can occur at a lower value of acceleration (.66g) if the frequency of vibration is high. This also depends on the duration of motion. This verifies D' Appolonia's¹⁰ observation on vibro-floatation. From the experimental observations, made earlier, it can be observed that there is a particular frequency of the soil motion at which the resistance to the sphere penetration is the least. The cases observed here, for the first sample

this critical frequency is 210 cps and for the second case, it is 170 cps, for the density and void ratio mentioned there in. It is worth mentioning that at lower frequencies the top surface of the soil behaves like a suspension upto a certain depth through which the ball can penetrate at a faster rate (Fig. 5.1) but ~~then it becomes~~ more or less stand still (velocity being extremely small). Thus the criterion for liquefaction during vibro-floatation can not be evaluated only emphasizing on critical acceleration but it should include the frequency and the duration of vibration, as well.

Based on the above informations, it is observed that a quantitative value of the soil behavior, namely kinematic viscosity of the soil, can be obtained. This kinematic viscosity will be useful in predicting the behavior of structural elements founded on soil as a result of soil vibration. In obtaining a quantitative value of the viscosity terms, the classical method¹ gives uncertain values which can not be correlated with the soil vibration. As such it depends only on the sinking velocity and independent of the nature of soil vibration. The proposed solution is directly from the Navier-Stokes equations neglecting convective acceleration terms and, hence, is more representative to the actual situation. Of course, for the present situation, where viscosity terms are much higher in comparison to the inertial terms in the

Navier-Stokes equations, the acceleration term is, a bit, insignificant but vibration of the soil medium has to be taken care off.

Theoretical investigations, presented in these studies have the following advantages;

- 1) The solution procedure reported, herein, for the accelerated motion of a sphere in an oscillating fluid, is simple and can be applied for computations for a wide range of parameters involved.
- 2) These results can be used for practical solutions of sedimentation in reservoirs, grain size analysis and evaluation of the parameters involved such as viscosity, density ratio etc.
- 3) Having established the stability of the numerical integration technique it can be applied for a general type of such problems.

REFERENCES

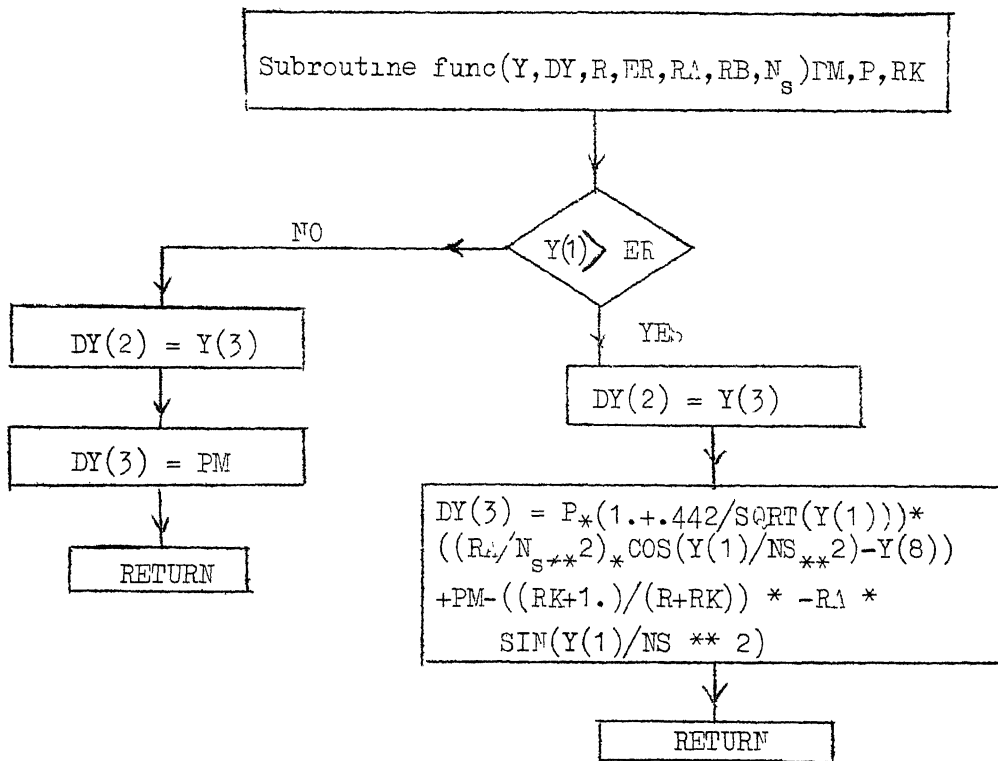
1. Barkan, D.D., "Dynamics of Bases and Foundations",
McGraw-Hill Book Company Inc. New York, 1960, pp.55-64.
2. Basset, A.B., "On the Motion of a Sphere in a Viscous Liquid"
Philosophical Transactions, Royal Society of London,
Vol. -43, 1898, p.179.
3. Basset, A.B., "A Treatise on Hydrodynamics", Vol.2, Dover
Publications, Inc. New York, 1961.
4. Batchelor, G.K., "The Skin friction on infinite cylinders
moving parallel to their length", Quarterly Journal of
Mechanics and Applied Mathematics, Vol. VII, Part II,
1954, p. 179.
5. Bateman, H., "Tables of Integral Transform", Vol. 1, McGraw-
Hill Book Company, Inc. New York, 1954.
6. Brush, L.M., Ho, H.W. and Yen, B.C., "Accelerated Motion of
a Sphere in a Viscous fluid", Journal of Hydraulic
Division, Proc. A.S.C.E., Vol. 90, No. HY 1, January,
1964.
7. Carslaw, H.S. and Jaeger, J.C., "The conduction of Heat in
Solids", Oxford University Press, Sec. 129, 1947.
8. Carstens, M.R., "Accelerated Motion of a Sphere", Ph.D.
Thesis, Iowa State University, Iowa, 1950.
9. Churchill, R.V., "Operational Mathematics", McGraw-Hill
Book Company, Inc. New York, 1958.

10. D'Appolonia, E., "Dynamic Loadings", Journal of Soil Mechanics and Foundations Division, Proc. A.S.C.E., Vol. 96, No. SM 1, January, 1970.
11. Florin, V.A. and Ivanov, P.L., "Liquefaction of Saturated Sandy Soils", Proceedings fifth International Conference on Soil Mechanics and Foundation Engineering, 1961, Vol. 1, pp. 107-111.
12. Hjelmfelt, A.T., and Mockros, L.F., "Stokes Flow Behaviour of an Accelerated Sphere", Journal of Engineering Mechanics Division, Proc. A.S.C.E., Vol. 93, No. EM6, December, 1967.
13. Huang-Wen-Xi, "Investigation Stability of Saturated Sand Foundation and Slopes Against Liquefaction", Proceedings, Fifth International Conference on Soil Mechanics and Foundation Engineering, 1961, Vol. II, p. 629.
14. Ho, H.W., "Fall Velocity of Sphere in a Field of Oscillating Fluid", Ph.D. Thesis, Iowa State University, Iowa, 196
15. Ishii, Arai, Y.H. and Tsuchide, H., "Lateral Earth Pressure in an Earthquake", Proceedings Second World Conference on Earthquake Engineering, Vol. 1, pp. 165-182.
16. Kishida, H., "Characteristics of Liquefied Sands During Mino-Owari, Tohnakai and FuKui Earthquakes", Soils and Foundations, Vol. IX, March, 1969, No.1, pp.75-92.
17. Lamb, H., "Hydrodynamics", Dover Publications, New York, 1945, pp. 642-644.

18. Lee, K.L. and Seed, H.B., "Cyclic Stress Conditions Causing Liquefaction of Sand", Journal of Soil Mechanics and Foundations, Proc. A.S.C.E., Vol. 93, No. SM 1, January, 1967, pp. 47-70.
19. Maslov, N.N., "Question of Seismic Stability of Submerged Sandy Foundations and Structures", Proceedings of the Fourth International Conference on Soil Mechanics and Foundation Engineering, Vol. 1, 1957, p. 365.
20. Matsuo, H. and Ohara, S., "Lateral Earthpressure and Stability of Quay Walls", Proceedings of the Second World Conference on Earthquake Engineering, 1960, Vol. 1, pp. 165-187.
21. Mogami, T., "Behaviour of Soils During Vibration", Proceedings of the Third International Conference on Soil Mechanics and Foundation Engineering, 1953, Vol. I, pp. 152-155.
22. Odar, F. and Hamilton, W.S., "Forces on a Sphere Accelerating in a Viscous Fluid", Journal of Fluid Mechanics, 1964, Part 2, Vol. 18, p. 302.
23. Ohsaki, Y., "Niigata Earthquake, 1964, Building Damage and Soil Condition", Soils and Foundations, 1966, Vol. VII, No. 2, pp. 14-37.
24. Ohsaki, Y., "Effects of Sand Compaction on Liquefaction During the Tokachioki Earthquake", Soils and Foundations 1970, Vol. X, No. 2, pp. 112-128.

25. Okamoto, S., "Bearing Capacity of Sandy Soil and Lateral Earthpressure during Earthquake", Proceedings of the First World Conference on Earthquake Engineering, 1960 Vol. 1, pp. 165-182.
26. Peacock, W.H. and Seed, H.B., "Sand Liquefaction Under Cyclic Loading Simple Shear Condition", Journal of Soil Mechanics and Foundations, Proc. A.S.C.E., 1968, Vol. 94, No. SM 3, pp. 689-708.
27. Prakash, S. and Mathur, J.N., "Liquefaction of Fine Sand Under Dynamic Loads", Proceedings of the Fifth Symposium of the Civil and Hydraulic Engineering Department, I.I.Sc., Bangalore, 1965, pp. B3/1-21.
28. Ralston, A. and Wilf, H., "Mathematical Methods for Digital Computers", John Wiley & Sons, Inc. New York, 1960, pp. 110-120.
29. Rayleigh, Lord, "On the Motion of Solid Bodies Through Viscous Liquid", Philosophical Magazine, 1911, Vol. XXI, pp. 697-711.
30. Seed, H.B. and Lundgren, "Investigation of the Effect of Transient Loading on the Strength and Deformation of Saturated Sands", Proceedings A.S.T.M., 1954, Vol. 45 p.1288.
31. Seed, H.B., and Lee, K.L., "Liquefaction of Saturated Sand During Earthquake", Journal of Soil Mechanics and Foundation, Proc. A.S.C.E., 1966, Vol. 92, SM6, PP 105-134.

32. Seed, H.B., and Idriss, I.M., "Analysis of Soil Liquefaction
Niigata Earthquake", Journal of Soil Mechanics & Foundation
Proc. A.S.C.E., 1967, Vol.93, SM3, pp. 83-108.
33. Sowerby, L., "The unsteady Flow of Viscous Incompressible
Fluid Inside an Infinite Channel", Philosophical
Magazine, 1951, Vol. 42, p. 176.
34. Taylor, D.W., "Fundamentals of Soil Mechanics", Asia
Publishing House, 1964.
35. Thomson, W.T., "Laplace Transformation", Longmans, Green
& Co., London, 1957.
36. Timoshenko, S., "Vibration Problems in Engineering",
D. Van Nostrand Company, Inc., Affiliated East-West
Press Pvt. Ltd., New Delhi, 1964.
37. Terzaghi, K., "Theoretical Soil Mechanics", Wiley, New York,
1943.
38. Yoshimi, Y., "An Experimental Study of Liquefaction of
Saturated Sands", Soils and Foundation, 1967, Vol.7,
pp. 20-32.
39. Yoshimi, Y., "An Out Line of Damage During the Tokachioki
Earthquake", Soils and Foundations, 1970, Vol. 10,
No.2, pp.1-14.



SUBROUTINE FUNC. FIGURE 6b.

NOTATIONS:

N : NO. OF DIFFERENTIAL EQUATION = 2
 H : STEP SIZE OF INDEPENDENT VARIABLE
 A,B,C : COEFFICIENTS IN THE RUNGE-KUTTA METHOD
 Y(1) : INDEPENDENT VARIABLE
 Y(2), Y(3): DEPENDENT VARIABLE
 Q(1),Q(2) : CORRECTIONS APPLIED TO EACH VARIABLE
 DY(1),DY(2) : DIFFERENTIAL EQUATIONS
 etc.

R = Density Ratio; RK = Added mass coefficient;
 RA = Amplitude of vibration to characteristic length ratio.
 RB = g/w^2L = Acceleration ratio
 $PM = ((R-1)/(R+RK)) * RB/NS^{**4}$
 $NS = SQRT(NEU/w*d^{**2})$ = Equivalent Stokes number
 $P = 18./(R+RK)$

APPENDIX - II

ACCELERATED MOTION OF A SPHERE IN AN OSCILLATING FLUID

The original derivation is due to Basset^{2,3}, who formulated the problem for the accelerated motion of a sphere in a stationary fluid under the action of gravity. To suit the problem discussed earlier, the following computational effort is made;

Let the sphere is of radius a , surrounded by a semi infinite fluid medium which is, let for the time being, at rest and sphere is moving with a velocity V . If squares and products of the velocity of the fluid are neglected, the current function ψ must satisfy the differential equation:

$$D \left(D - \frac{1}{\gamma} \frac{d}{dt} \right) \psi = 0 \quad \dots (1)$$

where

$$D = \frac{d^2}{dr^2} + \frac{\sin \theta}{r^2} \frac{d}{d\theta} \left(\text{Cosec} \theta \frac{d}{d\theta} \right), \text{ and the } (r, \theta)$$

are polar co-ordinates of a point referred to the center of the sphere as origin.

Now, in a single degree-of-freedom system, the velocity distribution function V can be written as, $V = \dot{x} - \dot{a}$, if the oscillation of the fluid be denoted as $a = a_0 \sin \omega t$, the terms were similar, as described in the Chapter III.

Let, R and θ be the components of velocities of fluid along and perpendicular to the radius vector, then, if we assume that no slipping takes place at the surface of the sphere, the surface condition,

$$R = \frac{1}{a^2 \sin \theta} \frac{d\psi}{d\theta} = V \cos \theta$$

$$\theta = - \frac{1}{a \sin \theta} \frac{d\psi}{dr} = - V \sin \theta, \text{ at infinity must vanish.}$$

If the impressed force is a constant force, here gravity, which acts in the direction of motion of sphere, and Z is the resistance due to fluid^{2,3},

$$Z = 2 \pi a \int_0^\pi (p a \sin \theta - \rho_f \frac{d\psi}{dt} \sin^2 \theta) a \sin \theta d\theta$$

Can be written as,

$$= - \pi \rho_f a \frac{d}{dt} \int_0^\pi (a \frac{d\psi_1}{dr} + 2 \psi_2) a \sin^3 \theta d\theta$$

$+ m_f g, \quad \psi_1, \psi_2, \text{ are the functions of}$

r and t ^{2,3}.

$$Z = - \frac{m_f}{a^2} \frac{d}{dt} (a \frac{d\psi_1}{dr} + 2 \psi_2) + m_f g$$

The term, $(a \frac{d\psi_1}{dr} + 2 \psi_2)_a$ reduces to ^{2,3}

$$-V \left(\frac{g}{2} \tau t + 9a \sqrt{\tau t/\pi} + \frac{a^2}{2} \right)$$

Now, t has to be changed to τ , V to $F' (t - \tau) d\tau$, and integrated the result with respect to τ from 0 to t and obtained; with $F(0) = 0$, where $F(t)$ is the variable velocity, and $F(0) = 0$ gives rise to $\dot{x} = \dot{a}$, i.e. $\dot{x} \Big|_{t=0} = a_0$ w,

$$\begin{aligned} Z &= \frac{m_f}{a^2} \frac{d}{dt} \left\{ V \left(\frac{g}{2} t + 9a \sqrt{\tau t/\pi} \right) + \frac{a^2}{2} + m_f g \right. \\ &= \frac{m_f}{a^2} - \frac{d}{dt} \int_0^t \left(\frac{g}{2} \tau + 9a \sqrt{\frac{\tau}{\pi}} \right) F'(t - \tau) d\tau \\ &\quad \left. + km_f \dot{V} + m_f g, \right\} \end{aligned}$$

The equation of motion can be written as (Equating all the forces involved);

$$\begin{aligned} m_s \ddot{x} + km_f \dot{v} + \frac{9 m_f}{a^2} \frac{d}{dt} \int_0^t F' (t - \tau) \left\{ \frac{1}{2} \tau + a \sqrt{\tau/\pi} \right\} d\tau &= m_f a \\ &+ (m_s - m_f) g \end{aligned}$$

... (2)

where dots and slash denote derivatives with respect to t , and partial derivative with respect to t , respectively.

Now, let us consider the integrals;

Integrating by parts,

$$\int_0^t F'(t-\tau) \left\{ \frac{1}{2} \gamma \tau + a \sqrt{\gamma \tau / \pi} \right\} d\tau = - F(t-\tau) \left\{ \frac{1}{2} \gamma \tau + a \sqrt{\gamma \tau / \pi} \right\} \Big|_0^t + \int_0^t F(t-\tau) \left(\frac{1}{2} \gamma + \frac{a}{2} \sqrt{\gamma / \pi \tau} \right) d\tau$$

Putting $F(0) = 0$,

$$\begin{aligned} &= \int_0^t F(t-\tau) d\tau \left(\frac{1}{2} \gamma + \frac{a}{2} \sqrt{\gamma / \pi \tau} \right) \\ \text{Thus, } \frac{d}{dt} &\int_0^t F(t-\tau) \left(\frac{1}{2} \gamma + \frac{a}{2} \sqrt{\gamma / \pi \tau} \right) d\tau \\ &= \int_0^t F'(t-\tau) \left(\frac{1}{2} \gamma + \frac{a}{2} \sqrt{\gamma / \pi \tau} \right) d\tau \\ &= \frac{1}{2} \gamma \int_0^t F'(t-\tau) d\tau + \frac{a}{2} \int_0^t \sqrt{\gamma / \pi \tau} F'(t-\tau) d\tau \\ &= \frac{1}{2} \gamma V + \frac{a}{2} \sqrt{\gamma / \pi} \int_0^t \frac{F'(\tau)}{\sqrt{t-\tau}} d\tau \end{aligned}$$

Now, equation (2) becomes,

$$\begin{aligned} m_s x + km_f \dot{V} + \frac{9m_f}{2a^2} \left\{ \gamma V + a \sqrt{\gamma / \pi} \int_0^t \frac{F'(\tau)}{\sqrt{t-\tau}} d\tau \right\} \\ = m_f \ddot{a} + (m_s - m_f) g \quad \dots (3) \end{aligned}$$

Which ultimately reduces to;

$$\begin{aligned}
 m_s \ddot{x} + km_f (\ddot{x} - \ddot{a}) - m_f \ddot{a} + 3\pi\mu d (\dot{x} - \dot{a}) \\
 + \frac{9 m_f}{a^2} \sqrt{\gamma/\pi} \int_0^t \frac{\frac{d}{d\tau} (\dot{x} - \dot{a})}{\sqrt{t - \tau}} d\tau
 \end{aligned}$$

where, $0 \leq \tau \leq t$... (4)

The equation 4 is the governing equation as used in equation 3.1 of Chapter III.

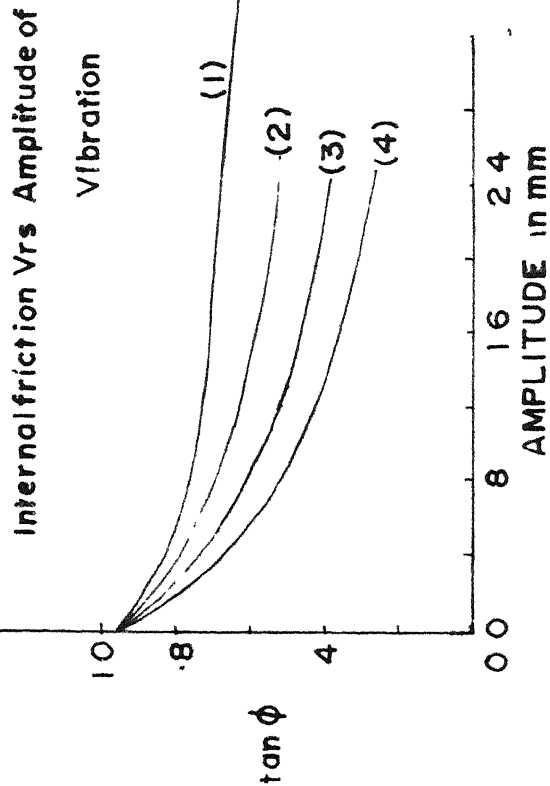


FIG 2.1

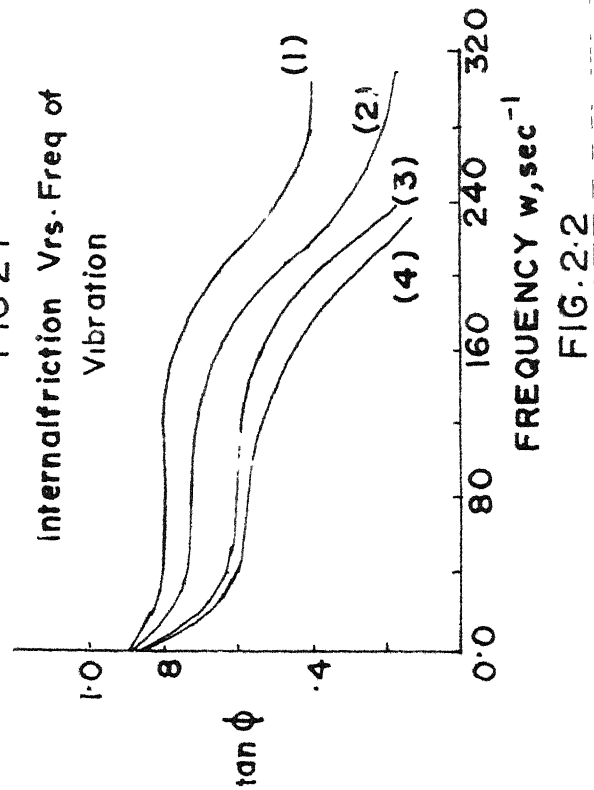


FIG. 2.2

(AFTER, BARKAN, 1960)

Effect of Vibration
Vrs.

Dia. of Sand grain

Variation of w ,

1 144 sec^{-1}

2 250 sec^{-1}

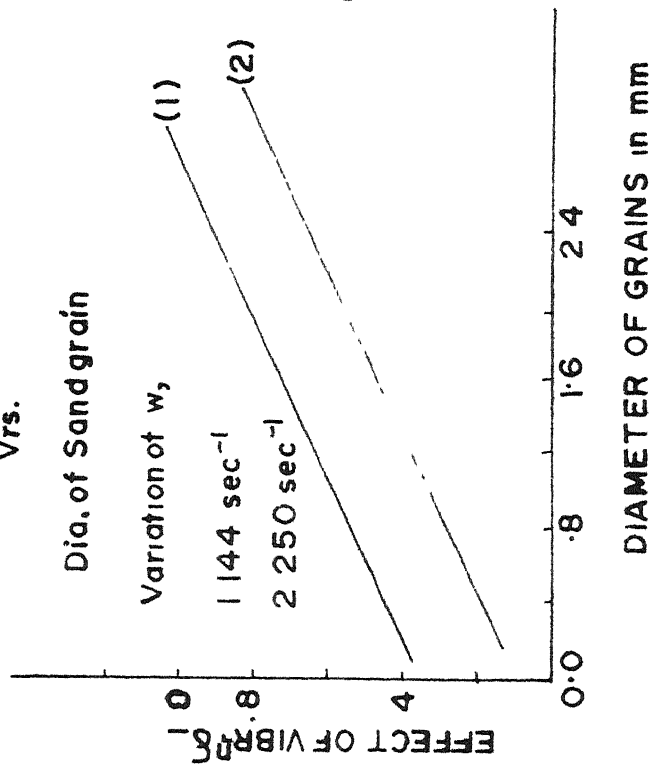


FIG 2.3

Variation of Amplitude
(FIG. 2.2)

1.0-35 mm

2.0-85 mm

3.12 mm

4.16 mm

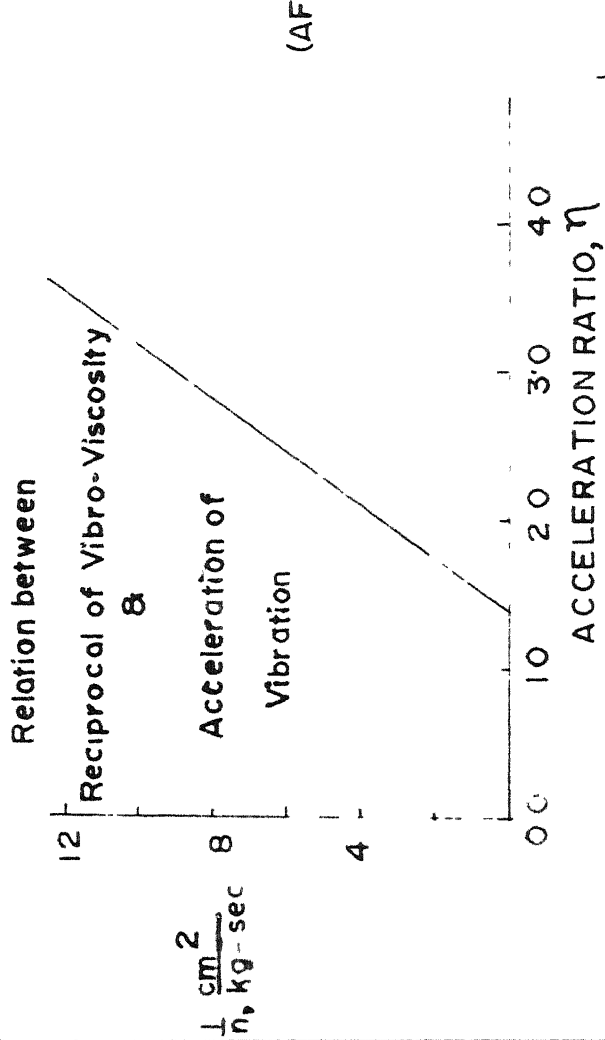
Variation of Freq.
(FIG 2.1)

1.25 sec^{-1}

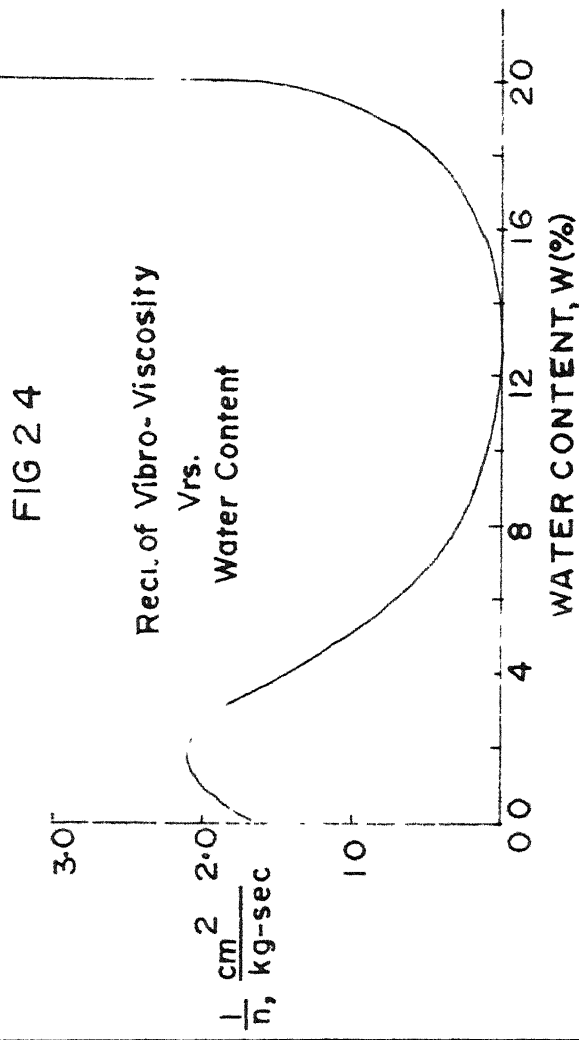
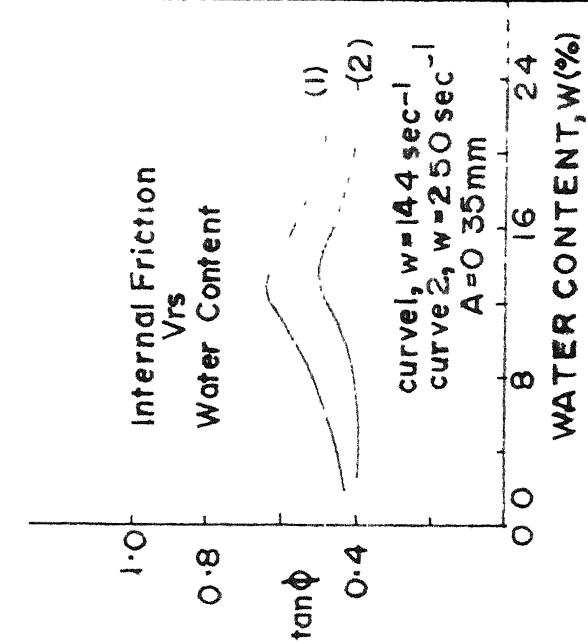
2.14 sec^{-1}

3.177 sec^{-1}

4.00 sec^{-1}



(AFTER, BARKAN, 1960)



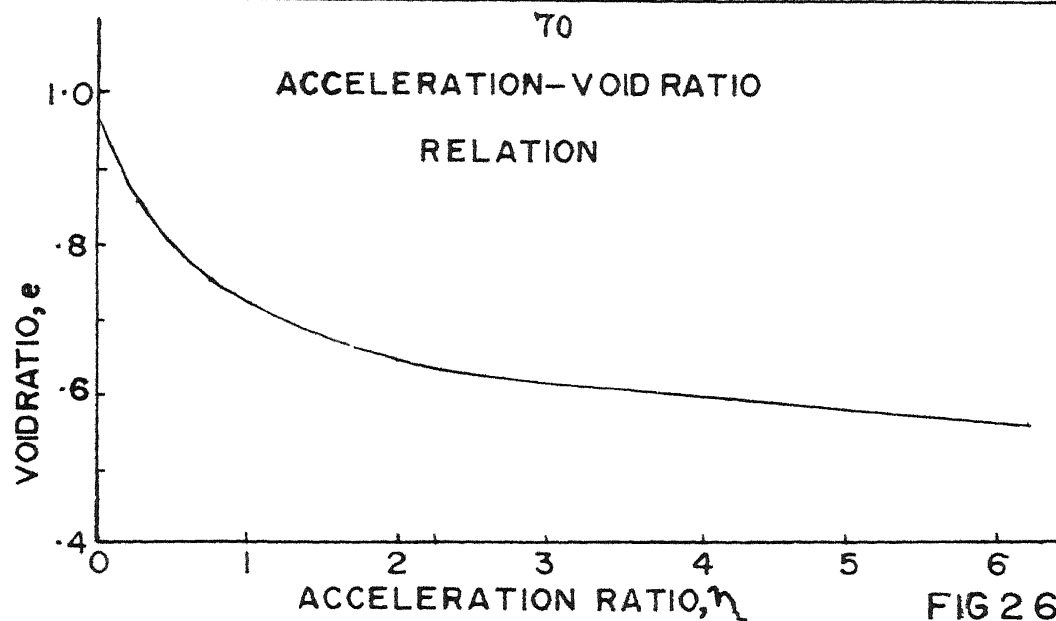


FIG 2 6
(After, BARKAN),
1960

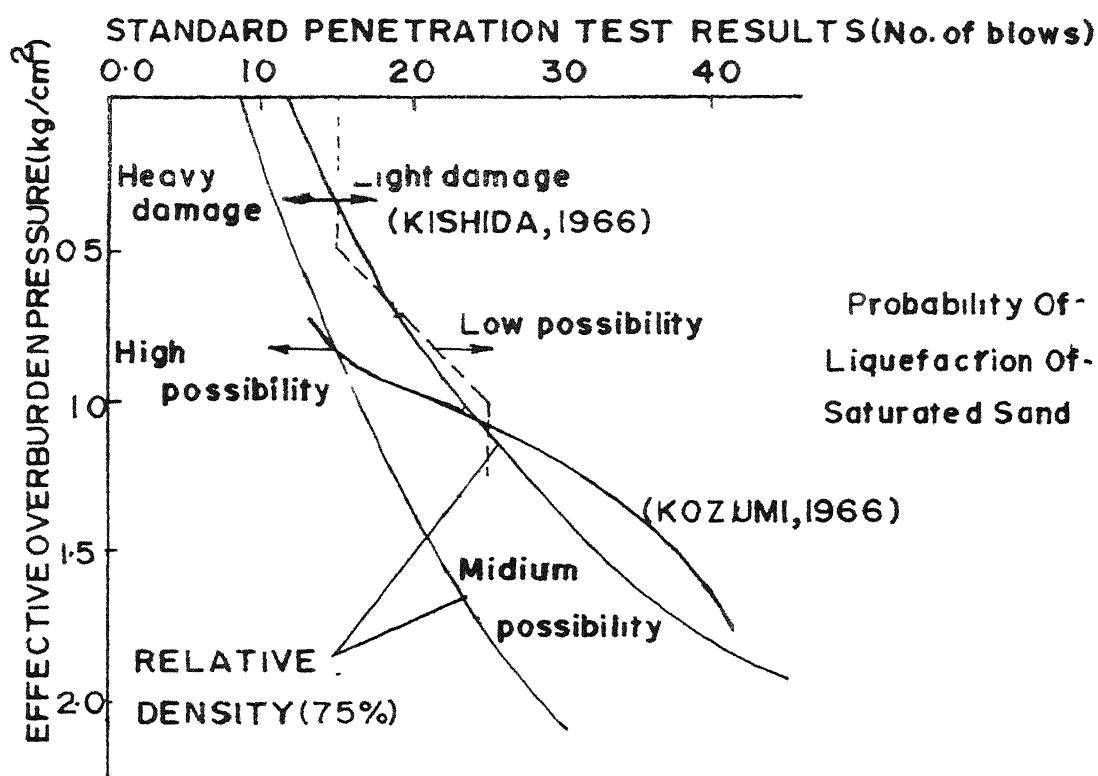


FIG.2.7

(AFTER, KISHIDA, 1969)

A. Proposed Solution
B. Carsten's Solution

$N_s=0.1$
 $RB=0.0001$
 $RA=0.0001$

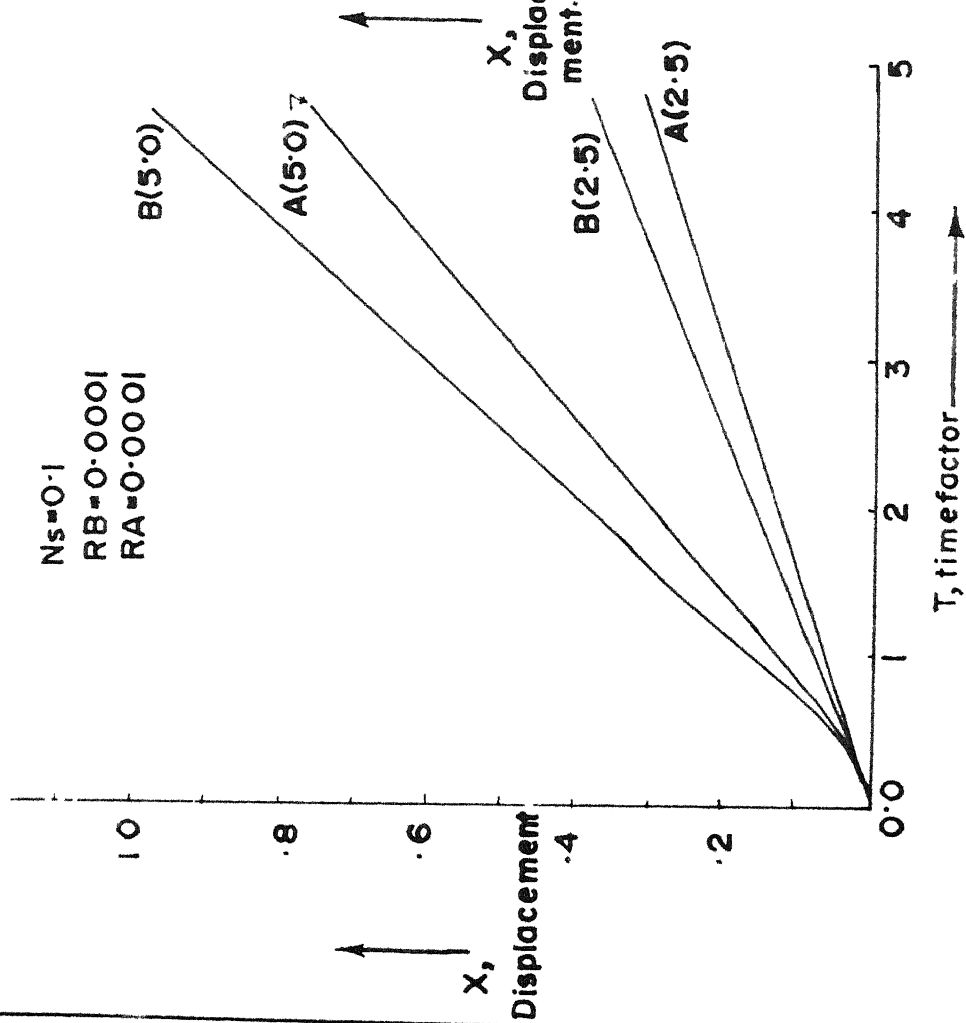
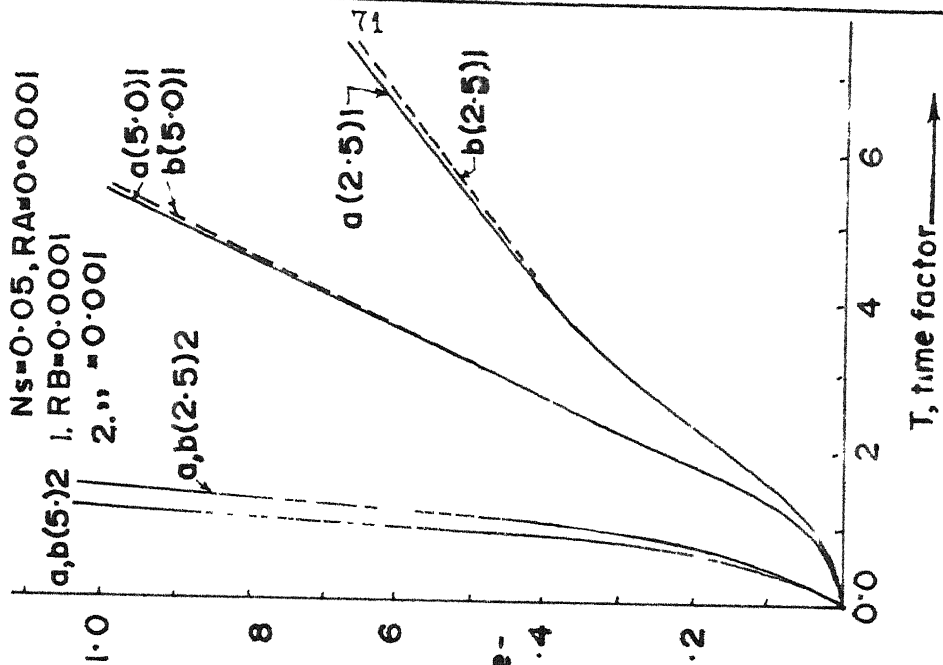


FIGURE 31

a. Stepsize, $H=0.02$
b Stepsize, $H=0.05$

$N_s=0.05$, $RA=0.0001$
 $RB=0.0001$
 $2.11=0.001$



Density ratios are shown under bracket

FIGURE 32 , Solution, varying H

A Proposed Solution

B Carsten's Solution

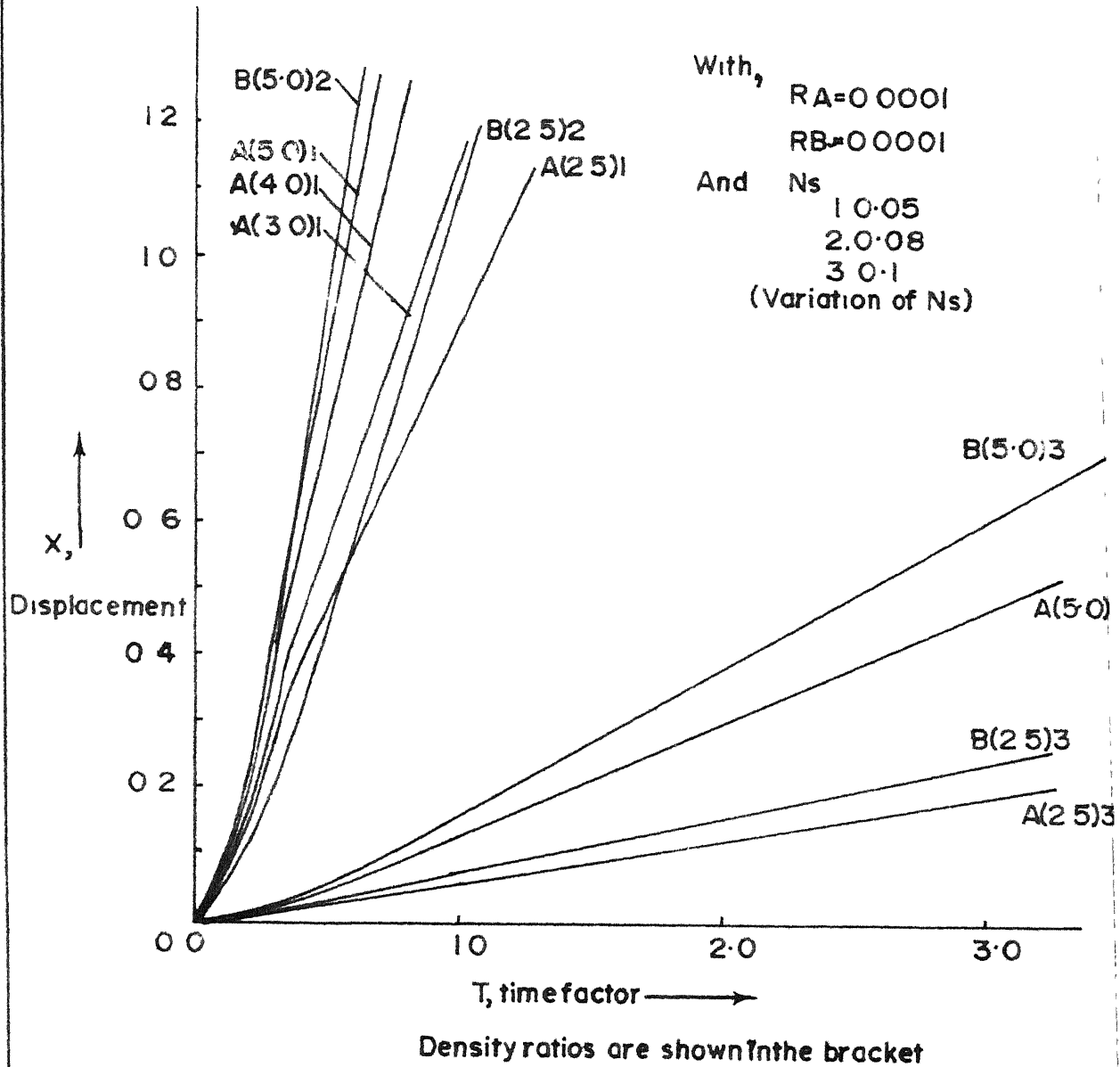
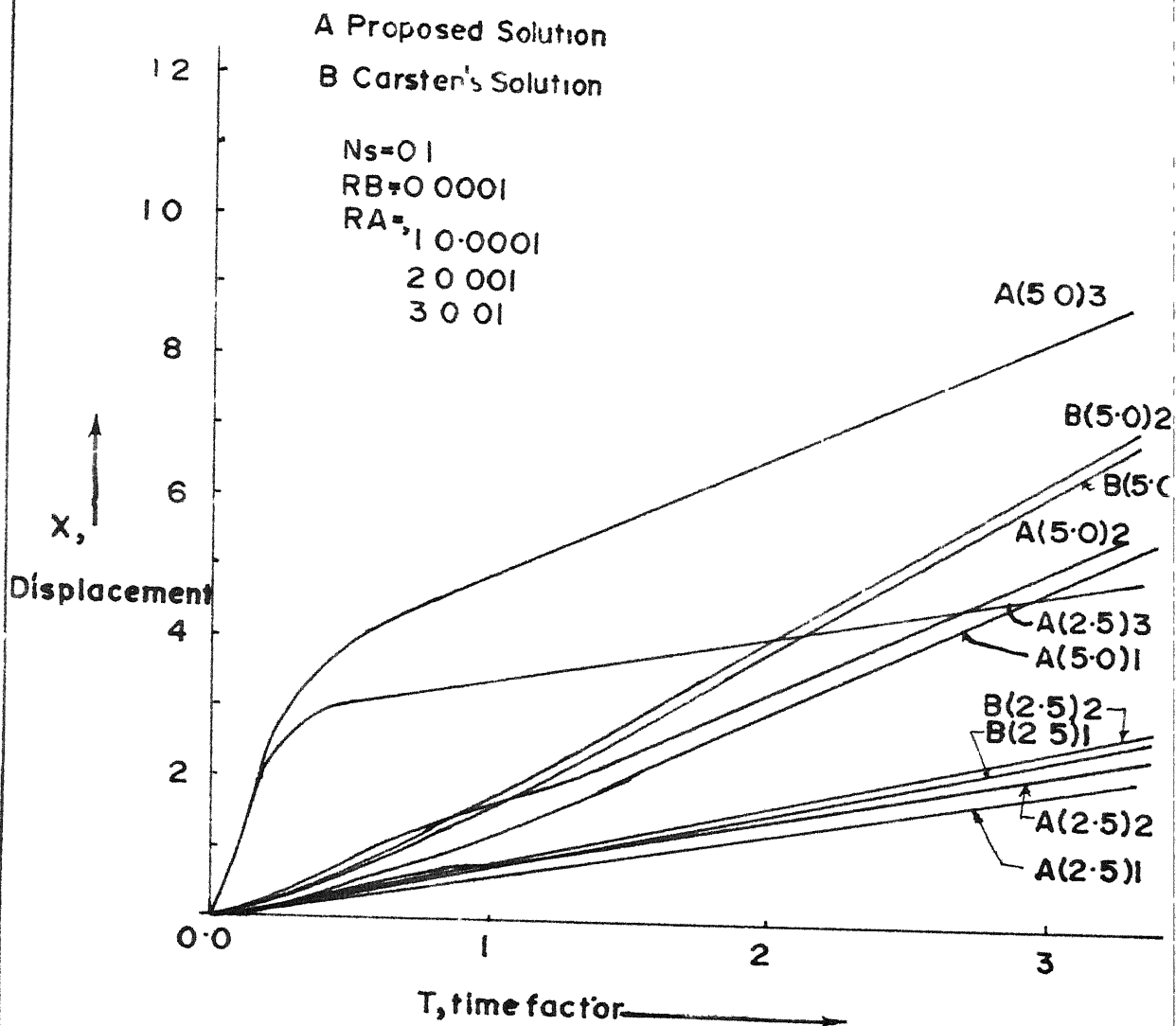


FIGURE. 3.3

VARIATION OF N_s .



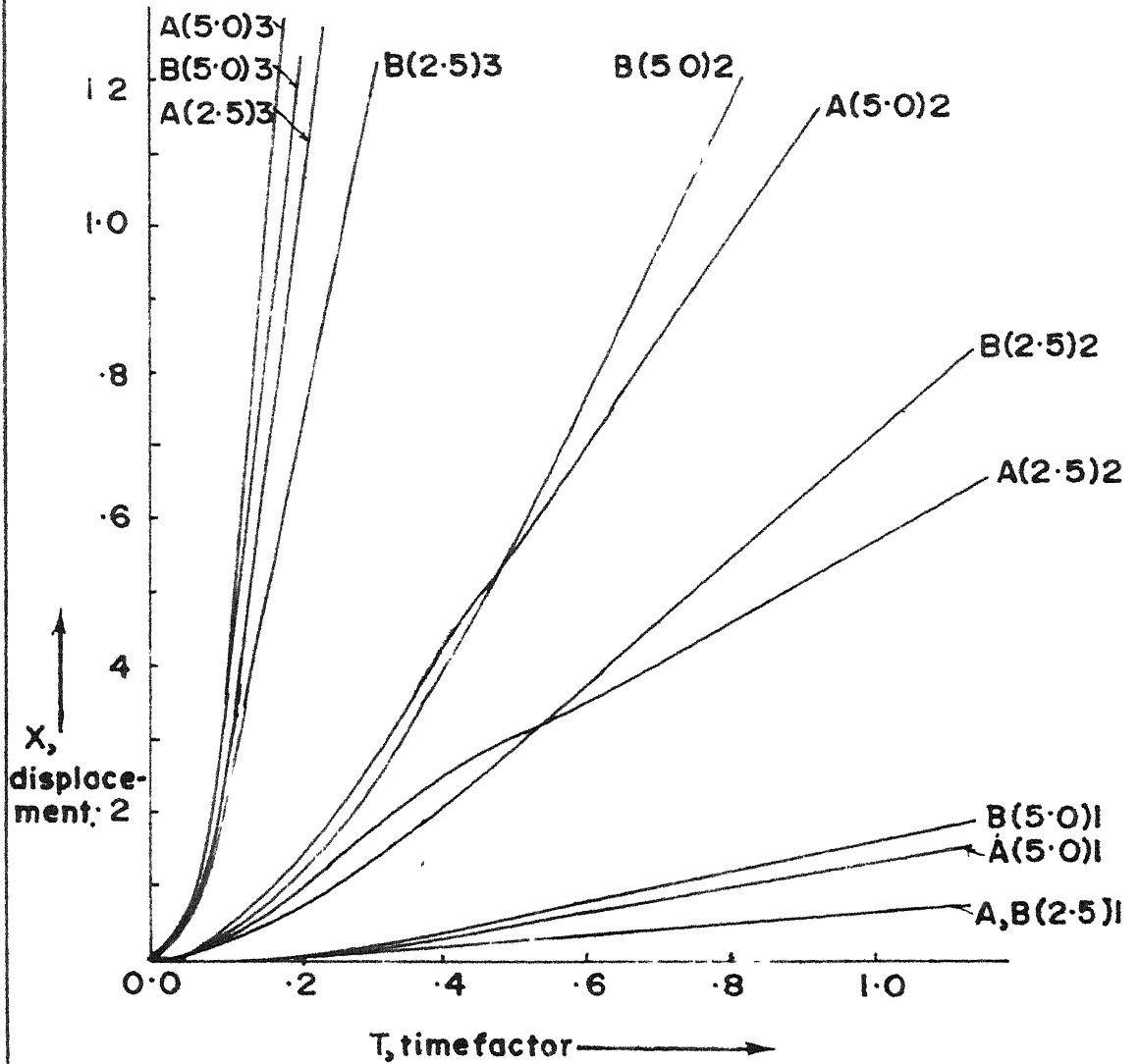
Density ratios are shown in the bracket.

FIGURE.3 4 , VARIATION OF RA

A Proposed Solution
B.Carsten's Solution

$N_s=0.1$, $RA=0.0001$

$RB=$,
1.0-0.0001
2.0-0.001
3.0-0.01



Densityratios are shown under bracket

FIGURE, 3 5 , VARIATION OF RB

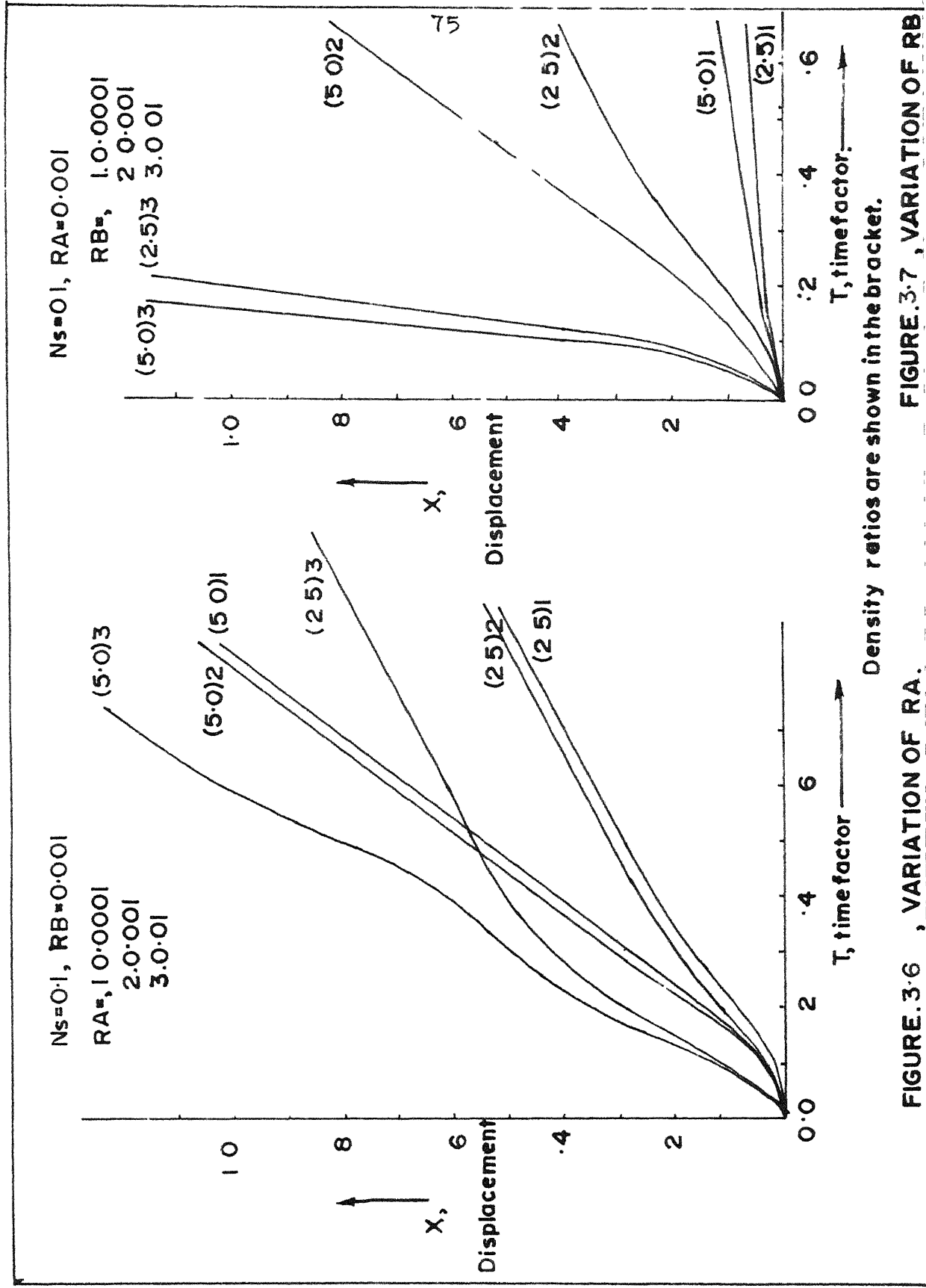


FIGURE.3.6 , VARIATION OF RA.

FIGURE.3.7 , VARIATION OF RB

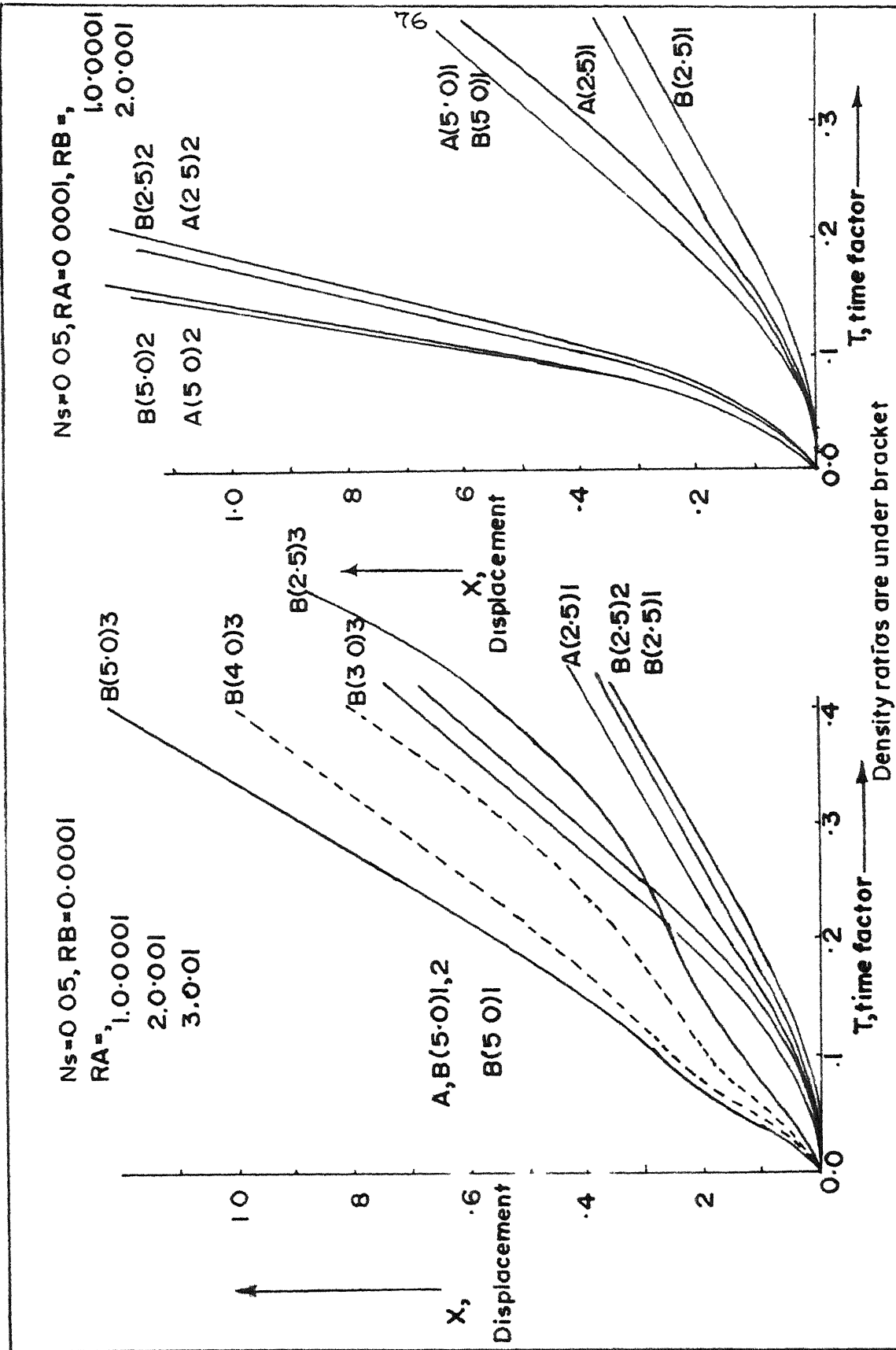
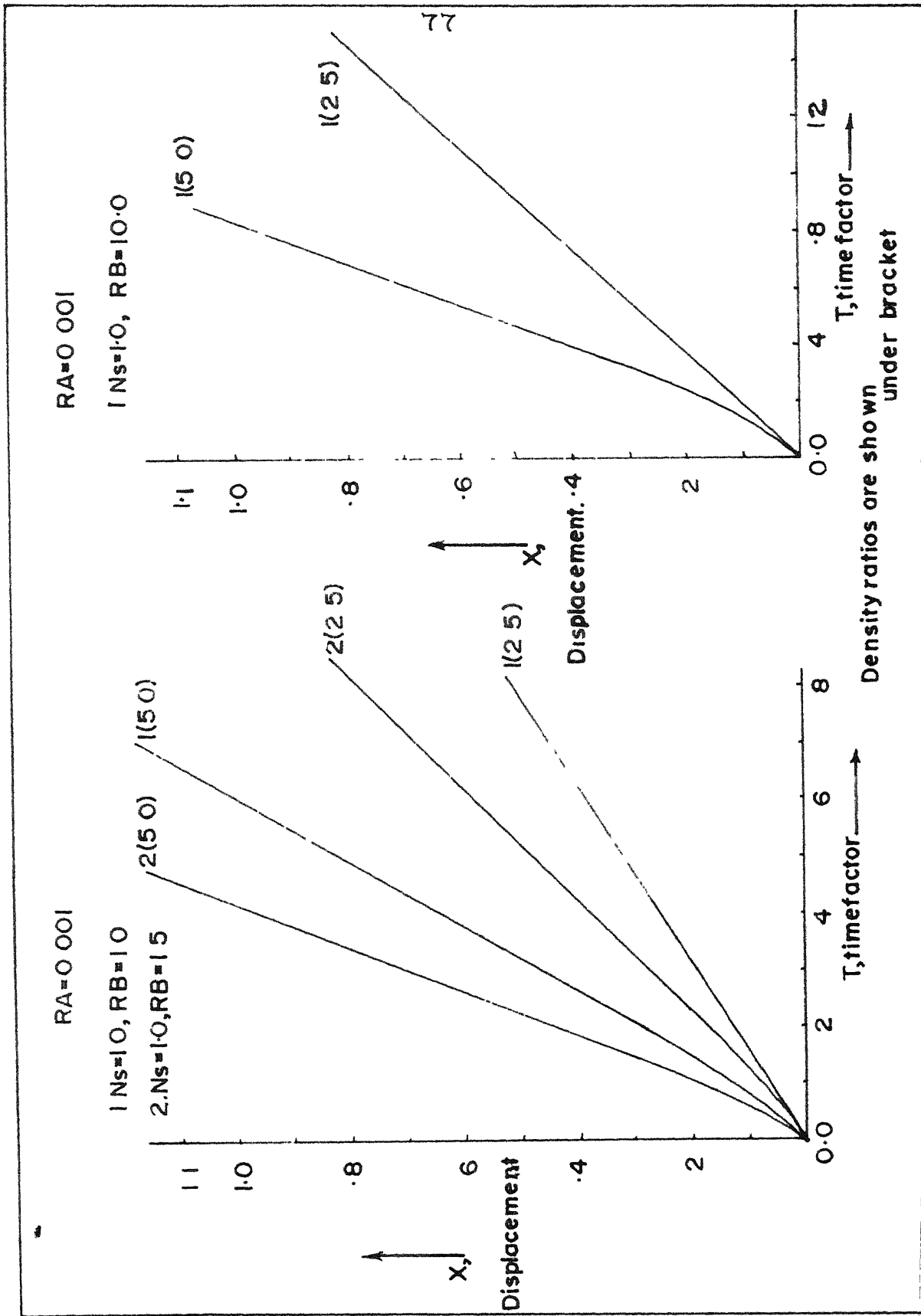


FIGURE 3.8, Variation of RA.

FIGURE 3.9, Variation of RB



COMPARISON WITH SOME EXISTING RESULTS

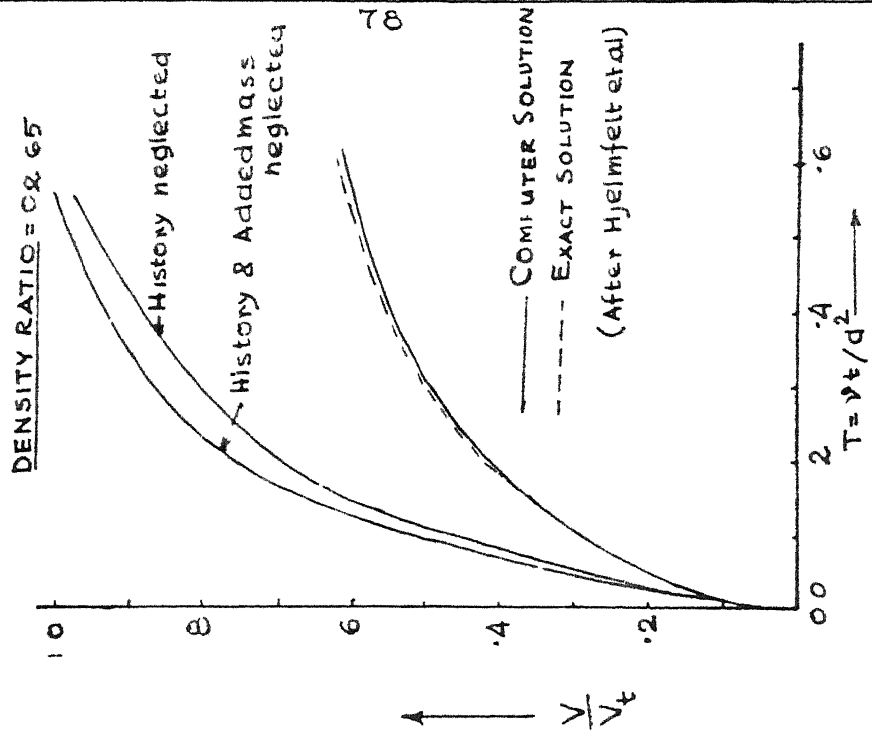


FIG 3.13

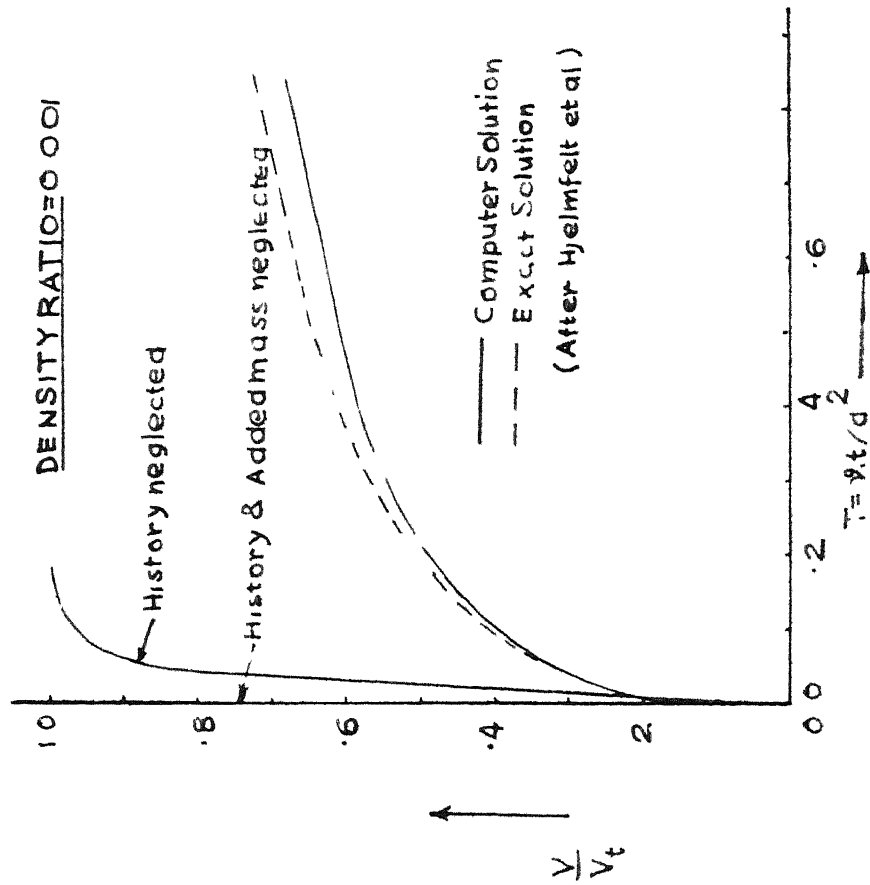


FIG 3.14

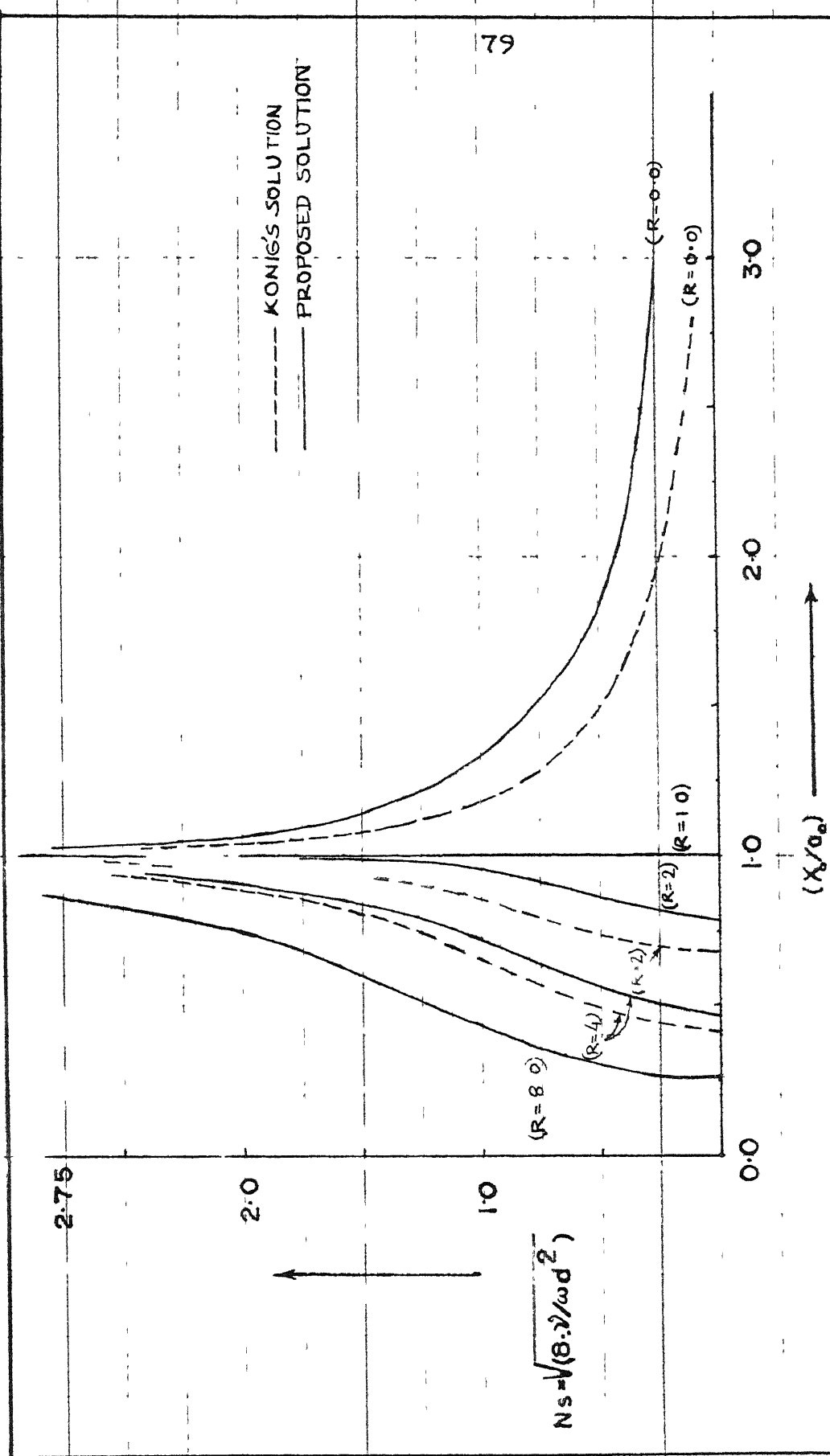
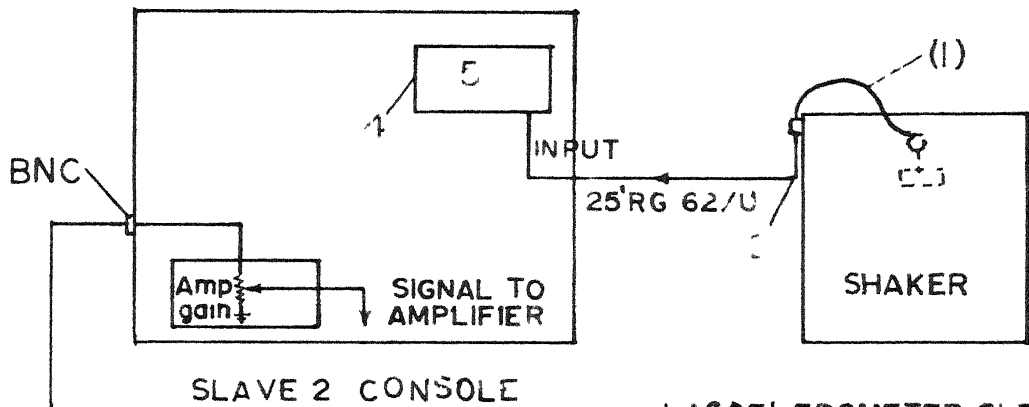
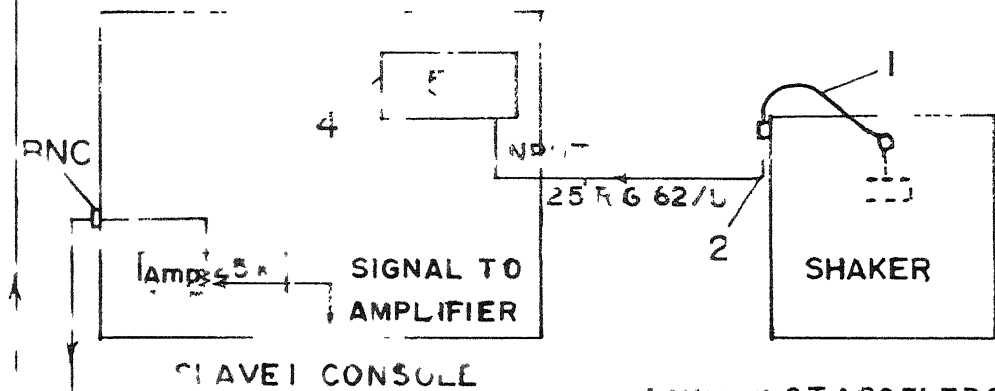


FIGURE 3.14 , A CHECK OF KONIG'S RESULT

(Density ratios are shown under bracket)



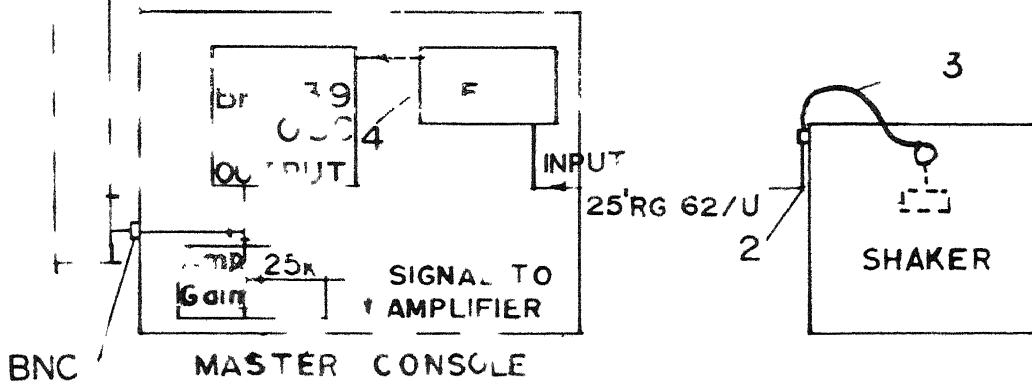
1 ACCELEROMETER CLEVITE 5021

2. MICRODOT TO BNC
CONNECT OR (33-

3. MICRODOT ACCELEROMETER CAE

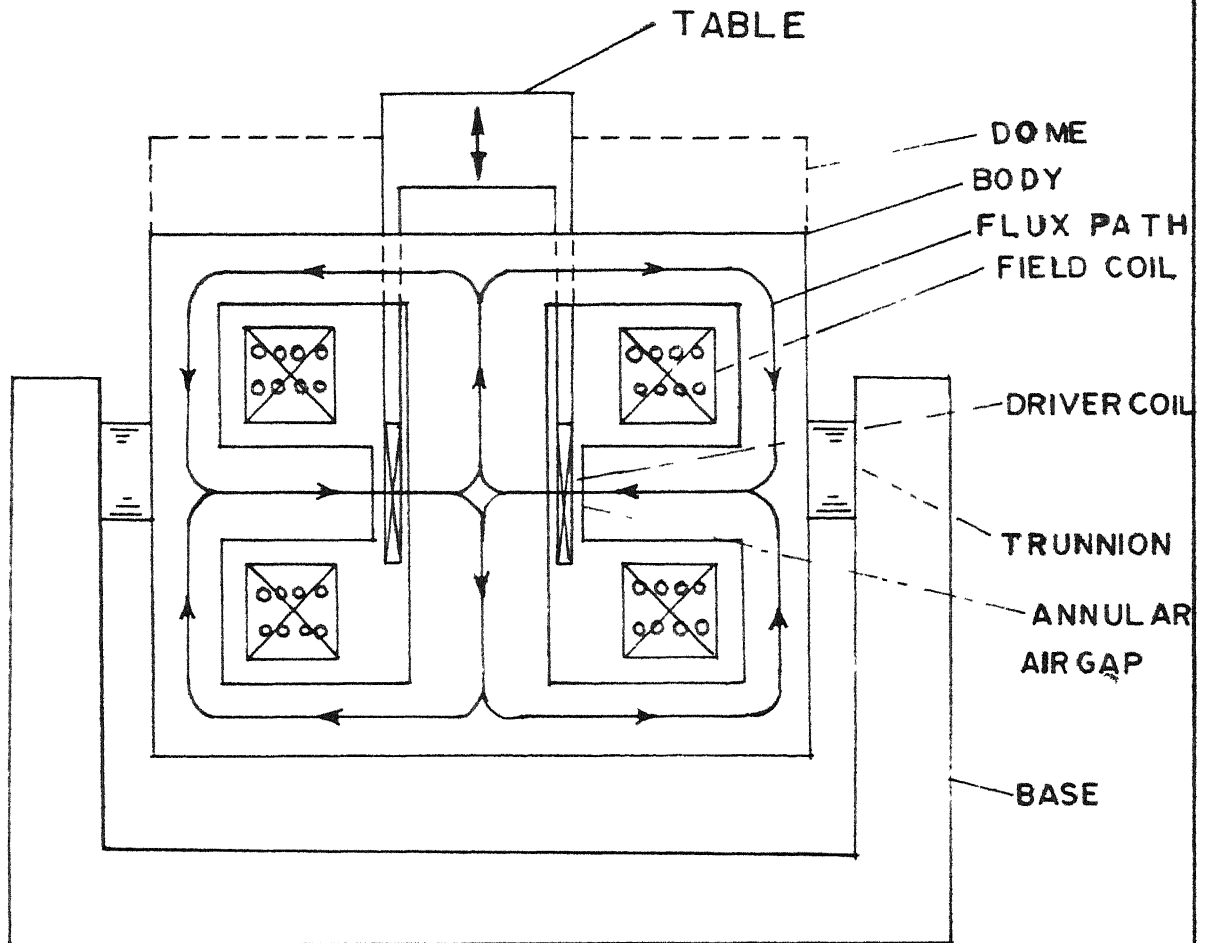
4 10mV(Peak) Per 'g' (Peak)

5 DIAL-A-GAIN 60 IR-A



INSTRUMENT INTERCONNECTION
(Reproduced from UNHOLT Z-DICKIE CORP Drawing No 9103269)

FIG. 41



SHAKER SCHEMATIC DIAGRAM

FIG.42

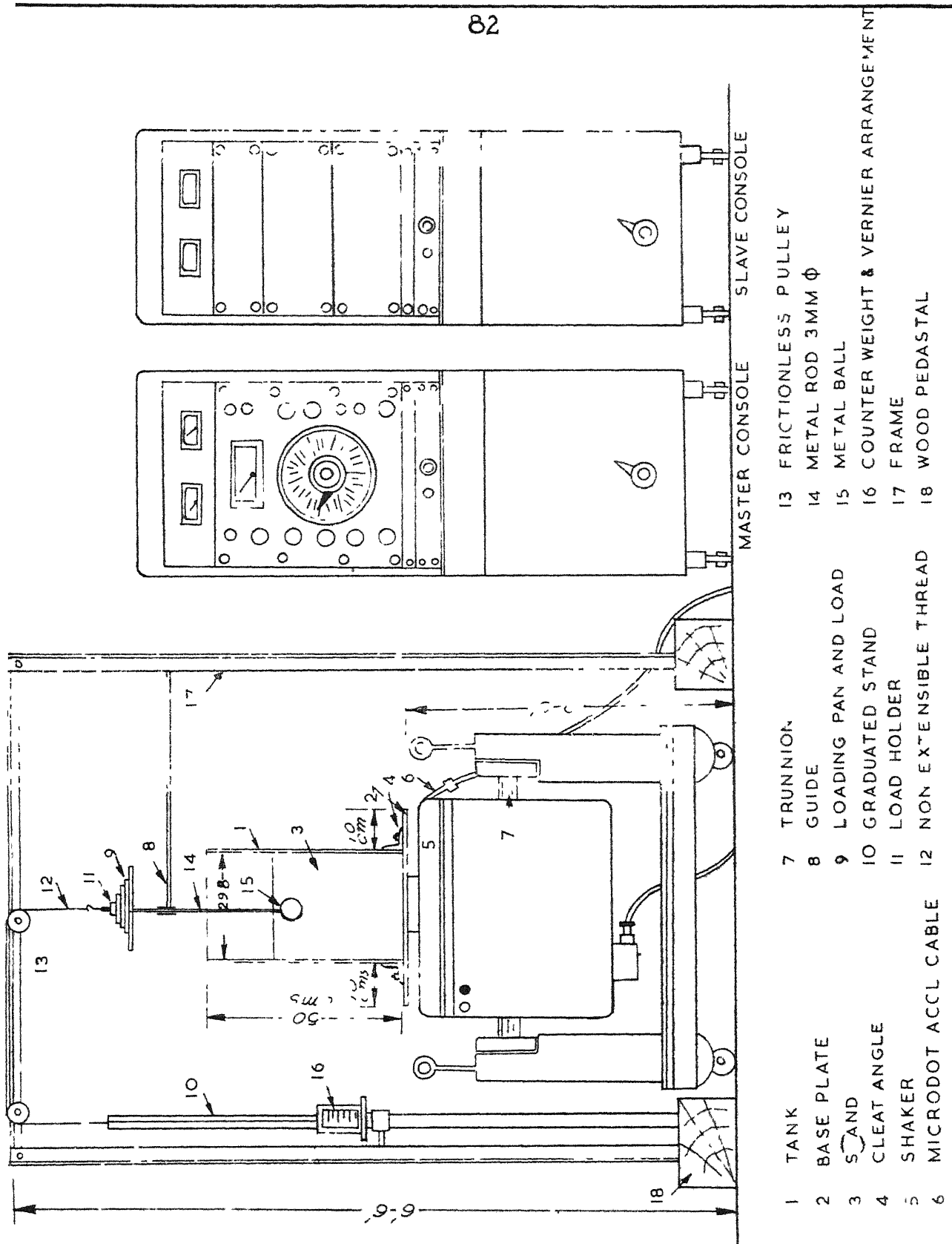
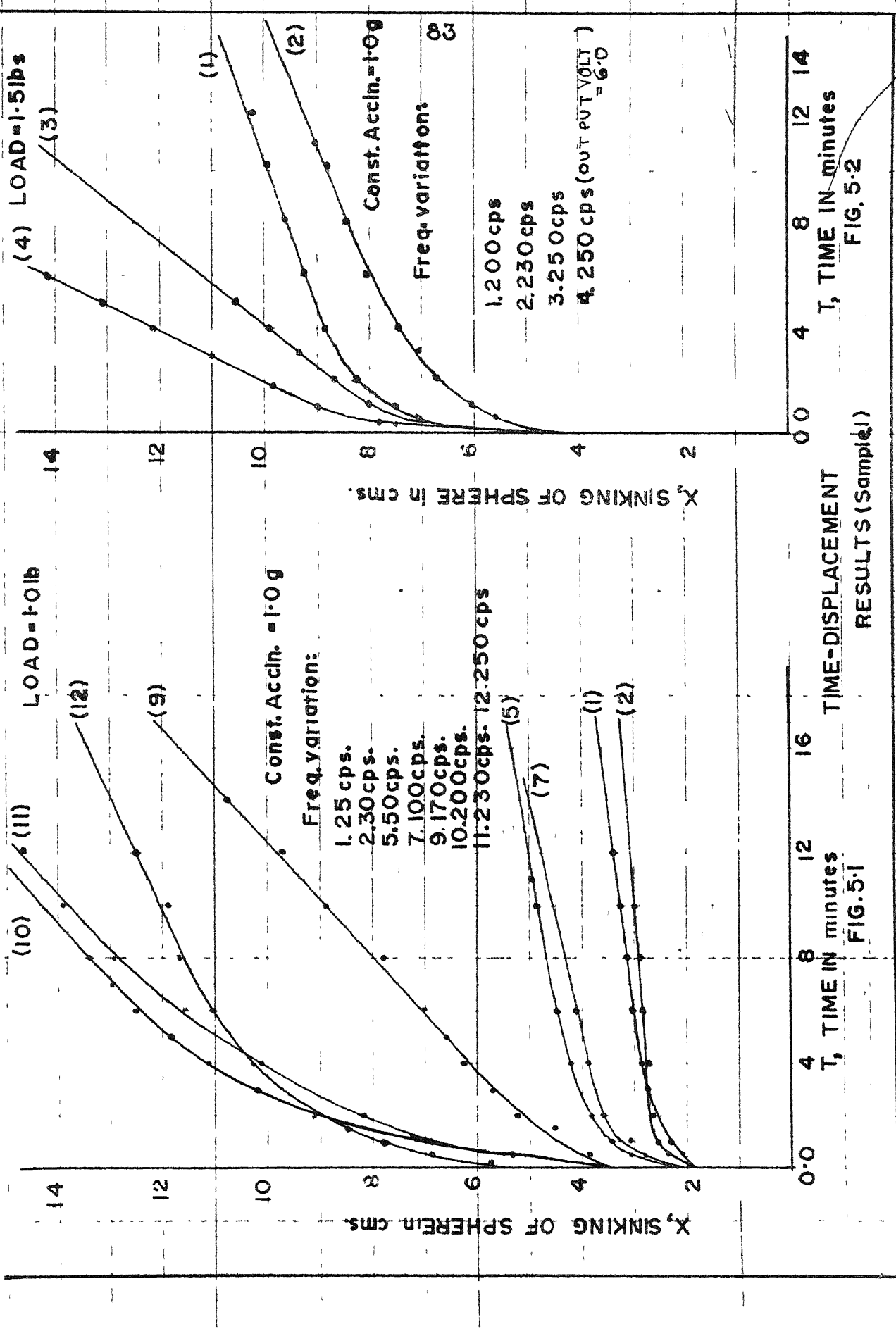


FIGURE.4.3.

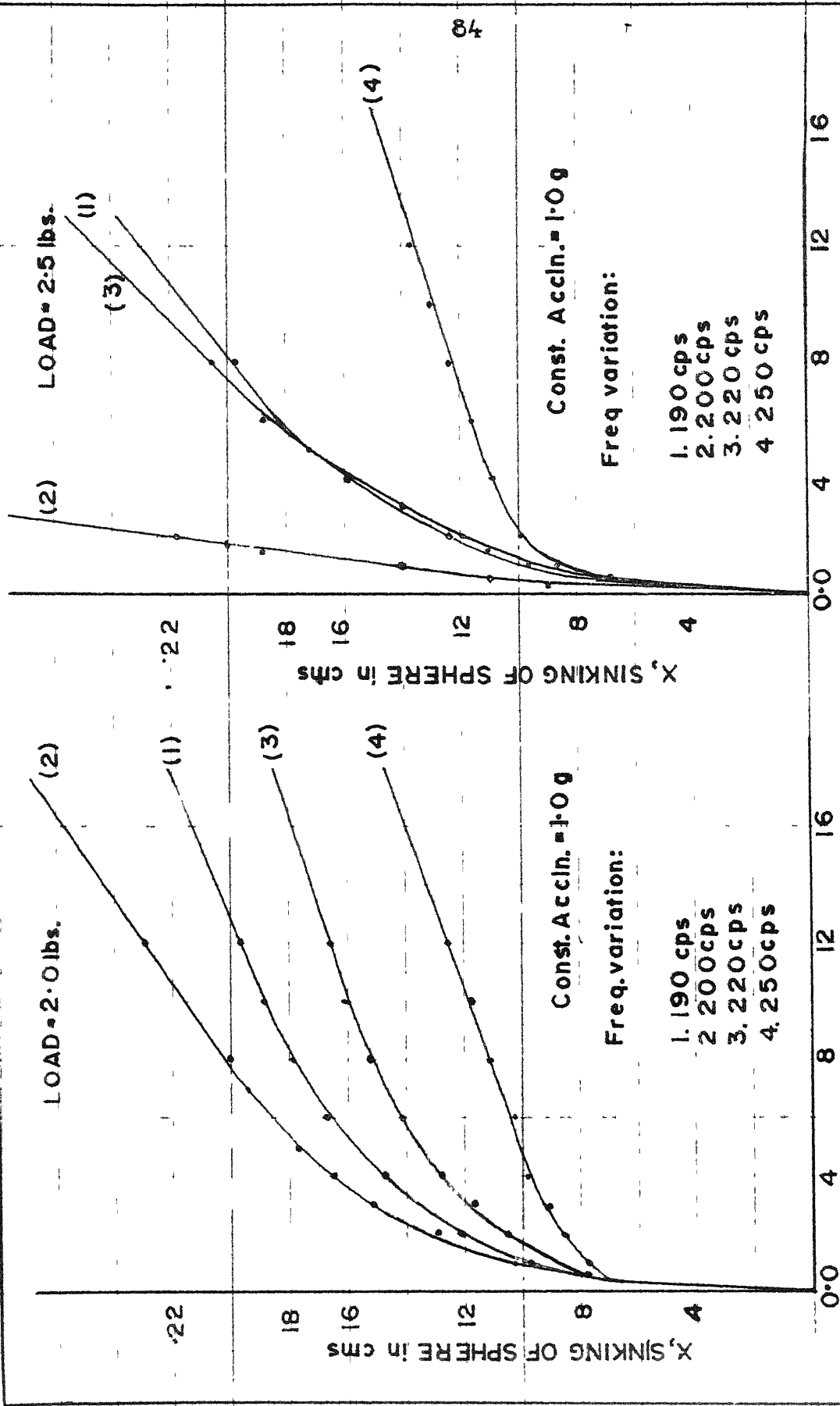
A SCHEMATIC DIAGRAM OF THE EXPERIMENTAL SET UP



RESULTS (Sample 1)

FIG. 5-2

FIG. 5-1



TIME-DISPLACEMENT
RESULTS (Sample 1)

FIG. 5.3

T, TIME in minutes

TIME-DISPLACEMENT
RESULTS (Sample 1)

FIG. 5.4

T, TIME in minutes

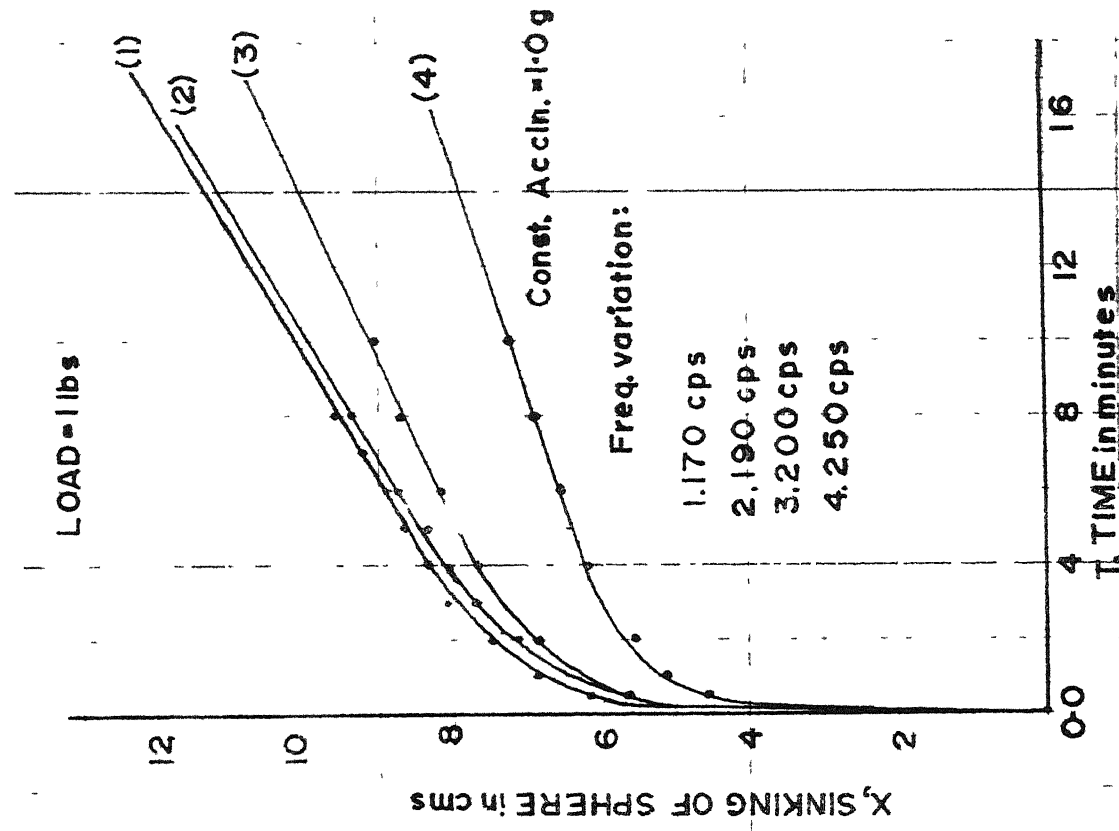
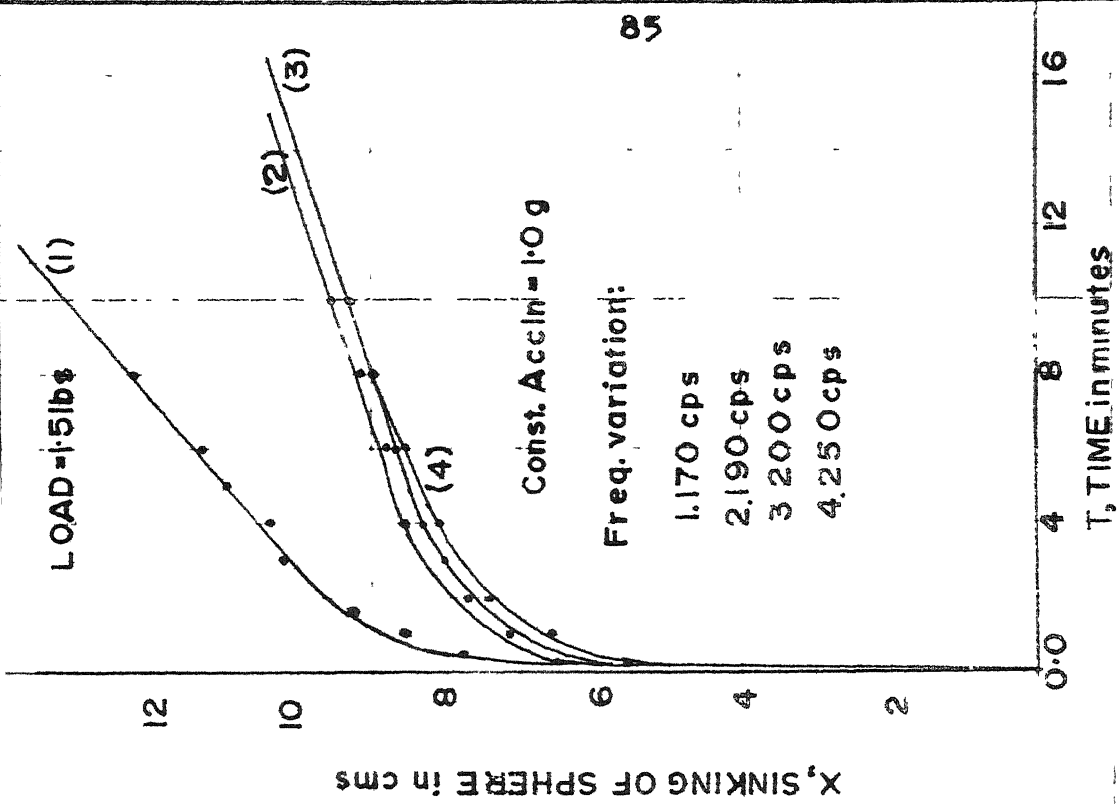


FIG. 5.8 RESULTS (Sample 2)

FIG 5.9

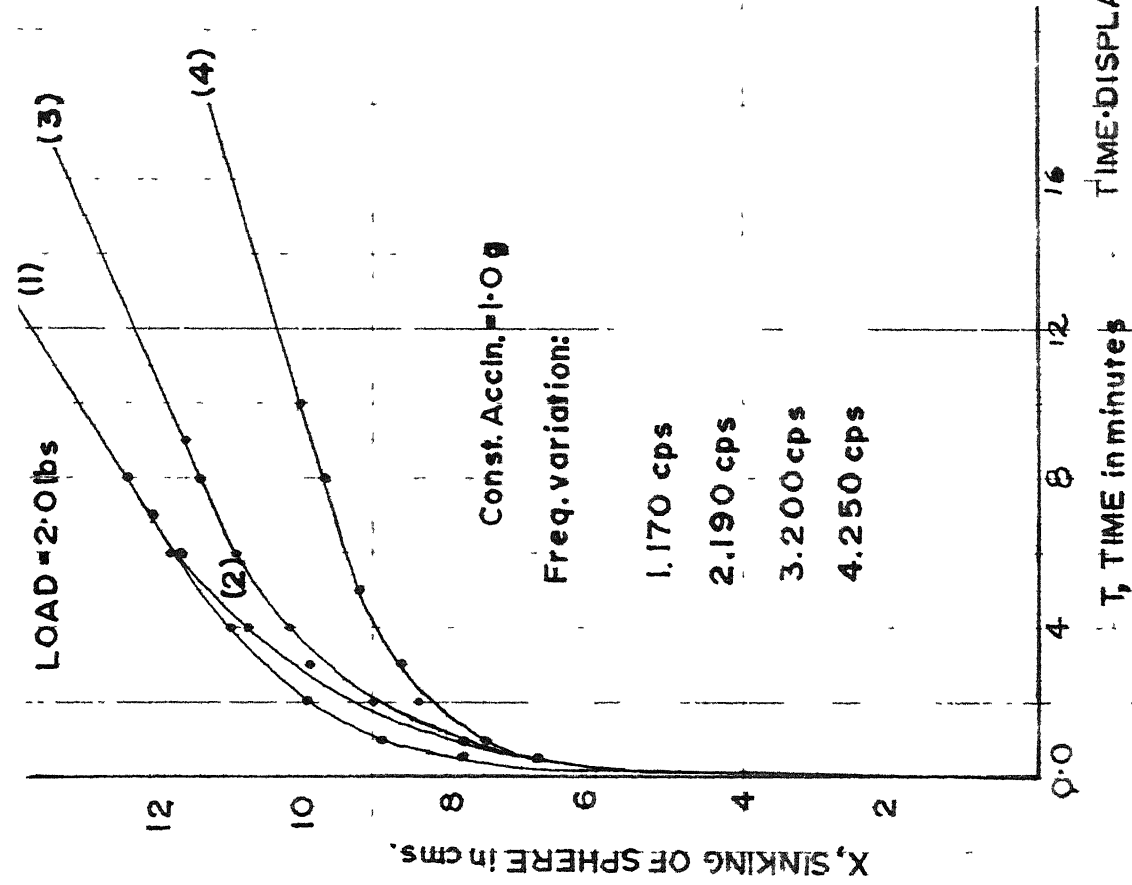


FIG. 510

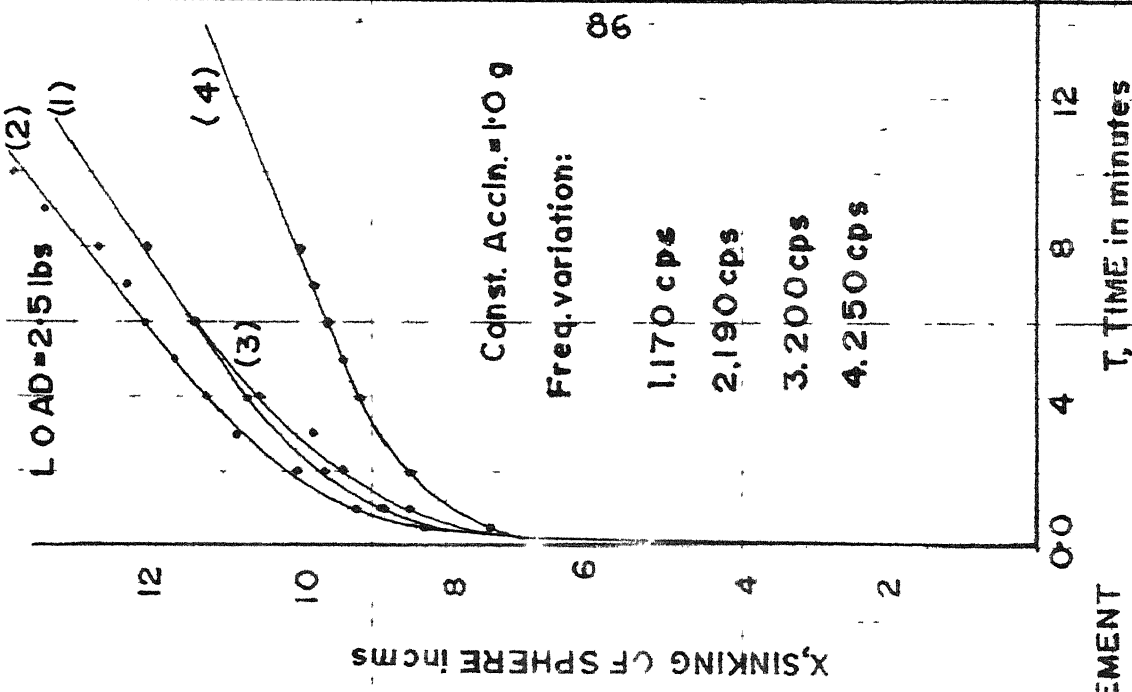


FIG. 511

RESULTS (Sample 2)

GRAINSIZE DISTRIBUTION CURVES

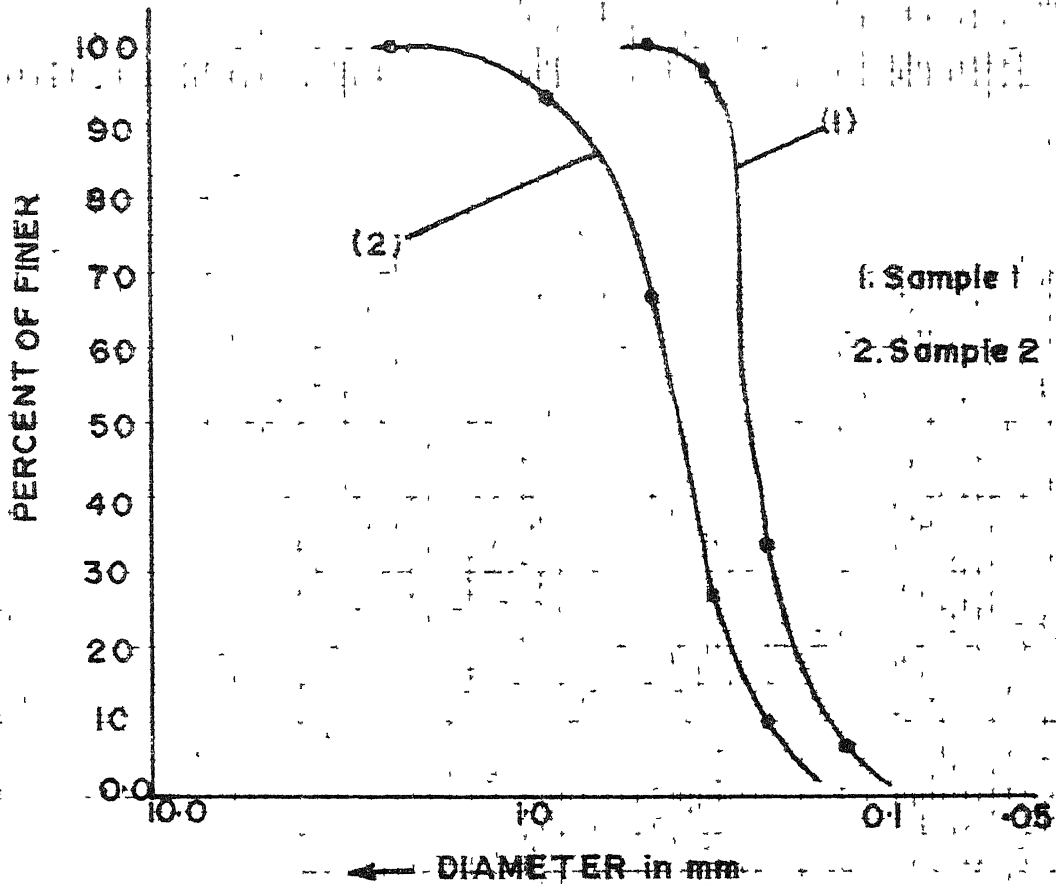


FIG. 5.12

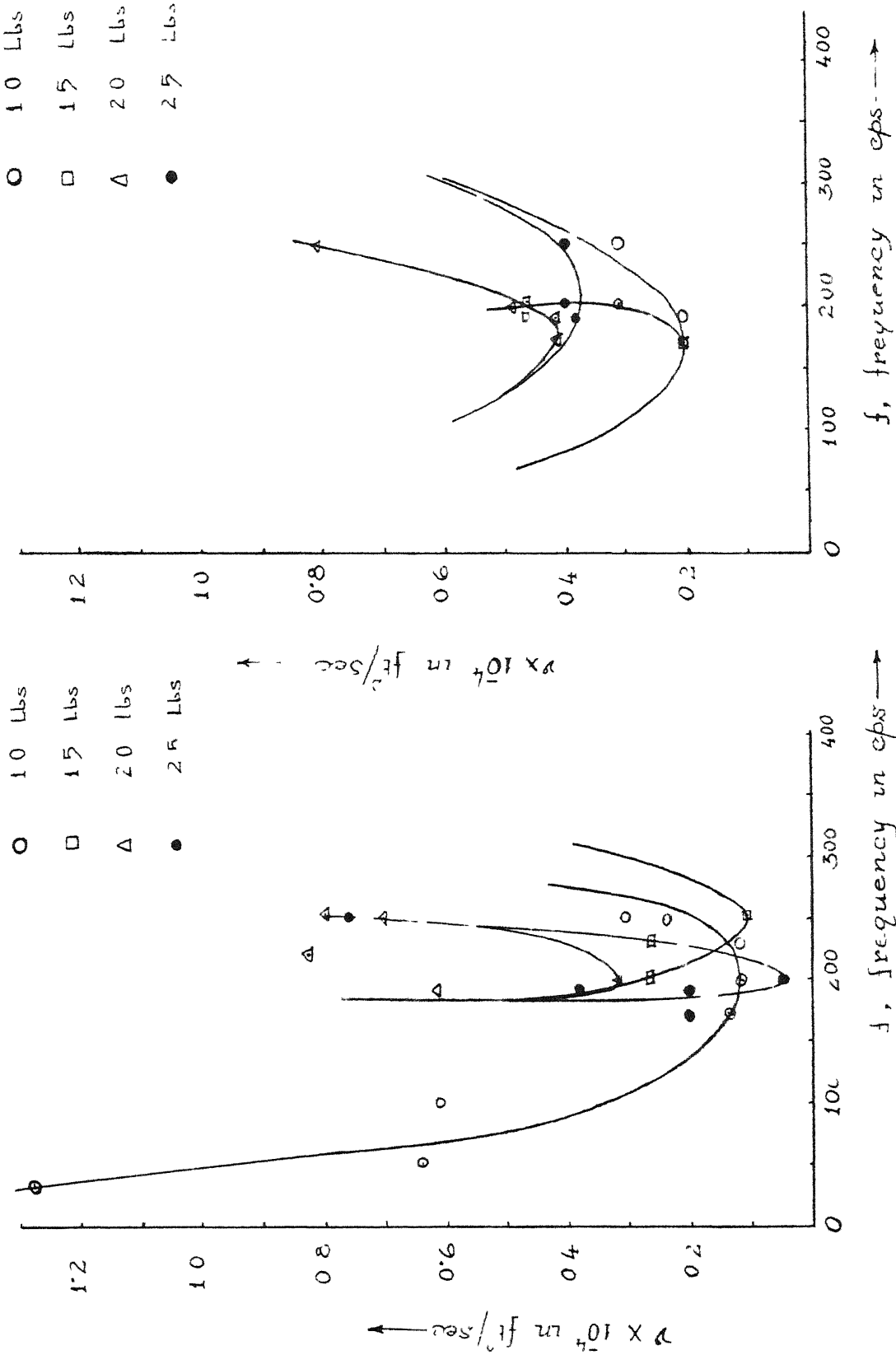


Figure 513a

variation of ν with frequency

Figure 513b

 f , frequency in cps \rightarrow

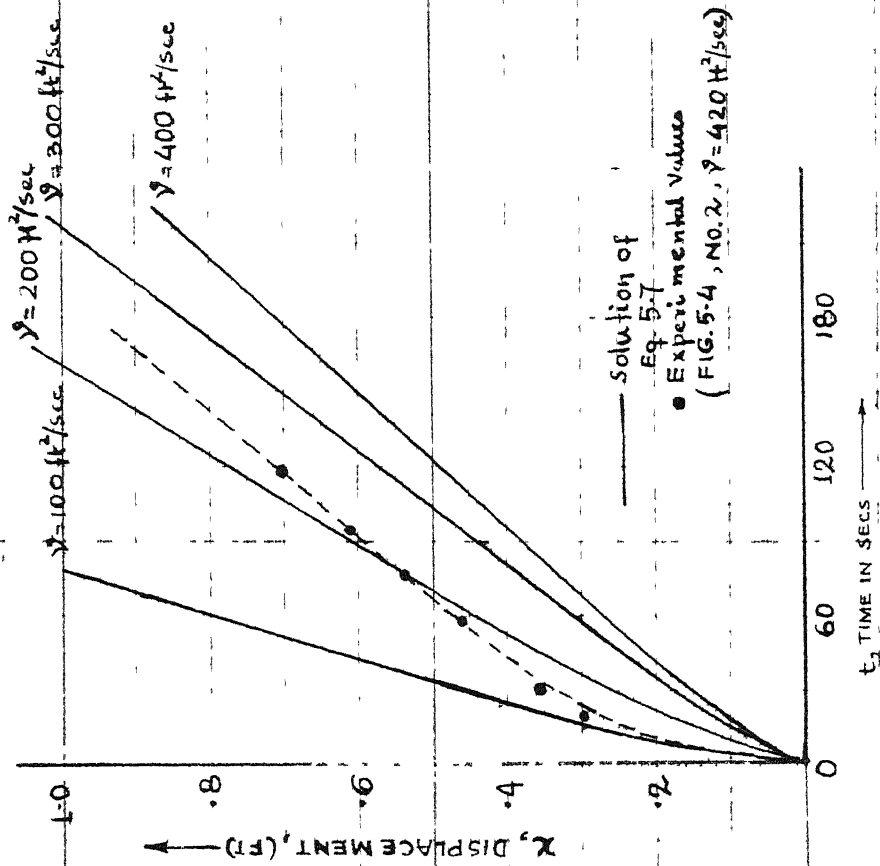


FIG 514

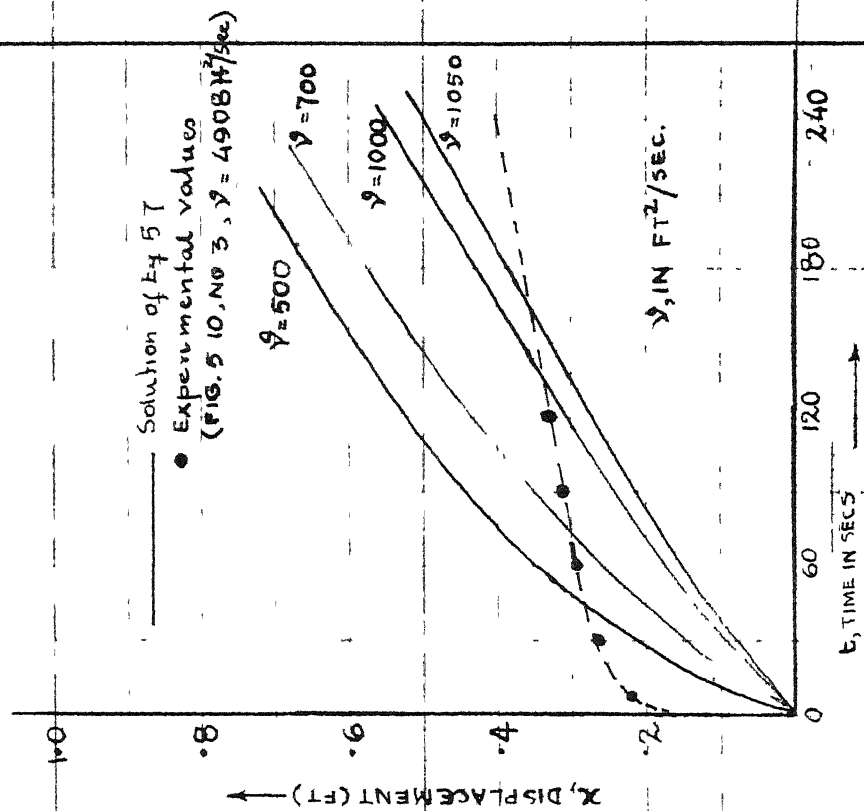
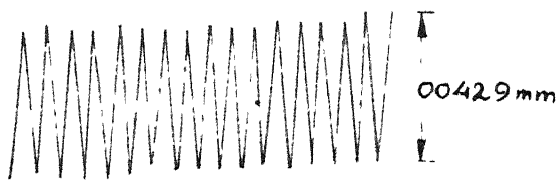
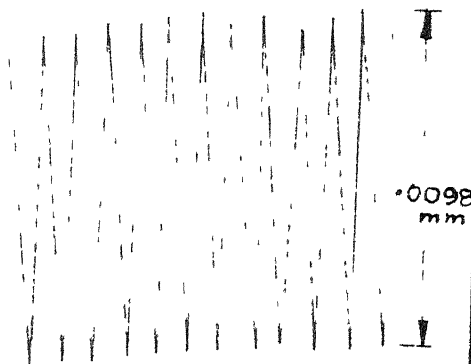


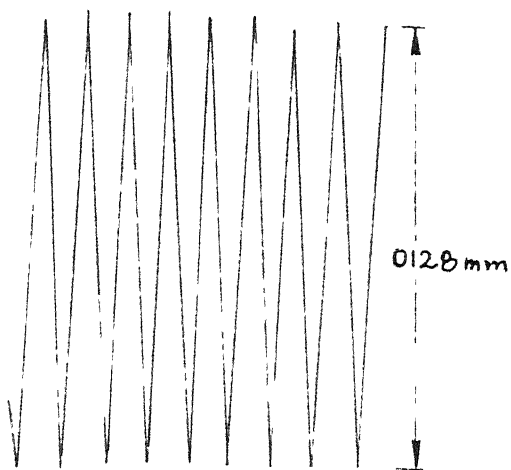
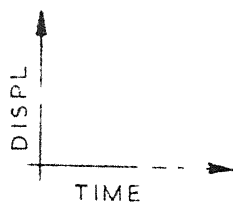
FIG. 5 15



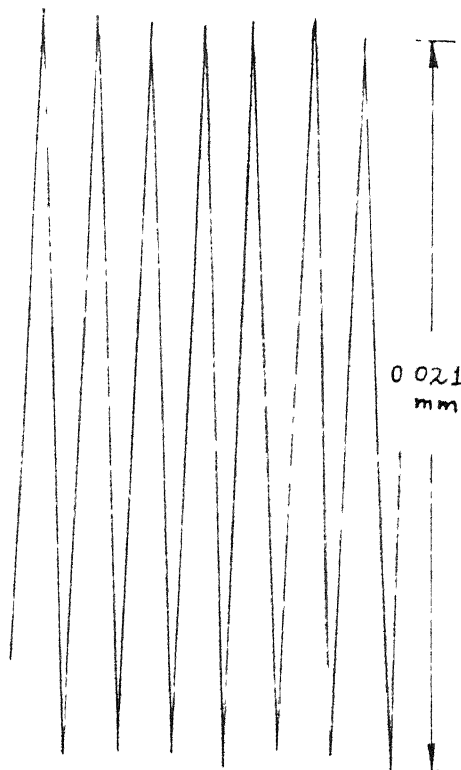
FREQ 150 CPS
(55)



FREQ 100 CPS
(55)

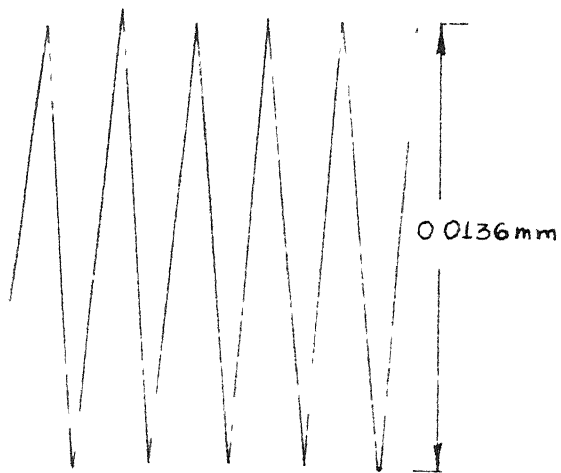


FREQ 70 CPS
(55)

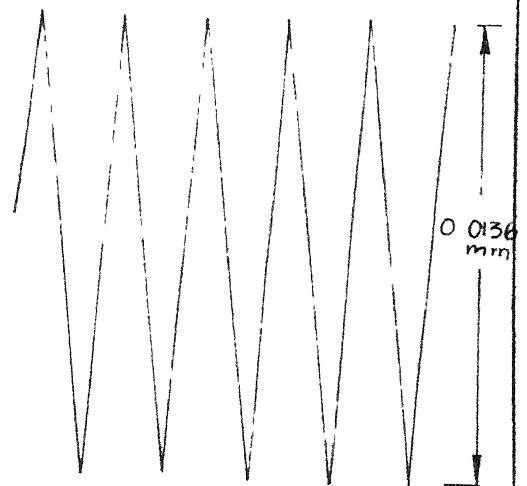


OUTPUT V. TRACES ARE SHOWN UNDER FREQ 50 CPS
BRACKET (55)

FIG 5 16 DISPLACEMENT VS TIME RESPONSE

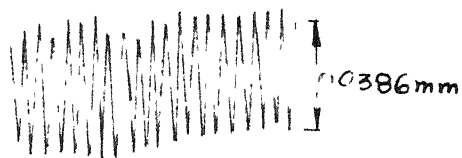


FREQ 30 CPS
(5.5)



FREQ 25 CPS
(5.5)

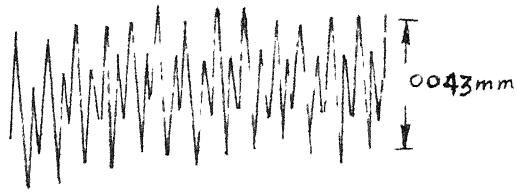
DISPL
↑
TIME →



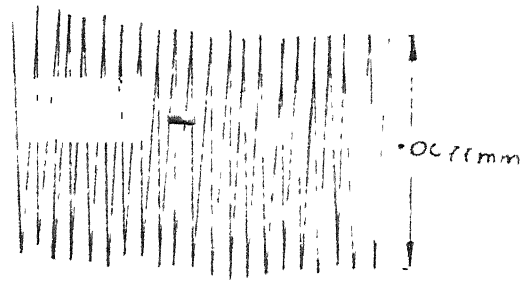
FREQ 250 CPS
(5.5)

OUTPUT VOLTAGE ARE SHOWN UNDER BRACKET

FIG 517 DISPLACEMENT VS TIME RESPONSE

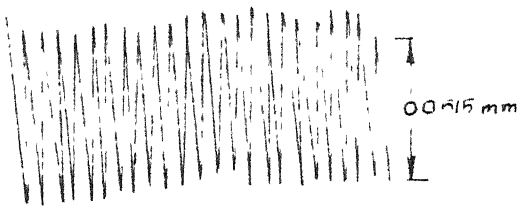


FREQ 250 CPS
(60)

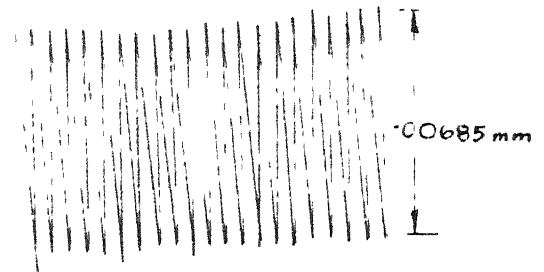


FREQ 200 CPS
(55)

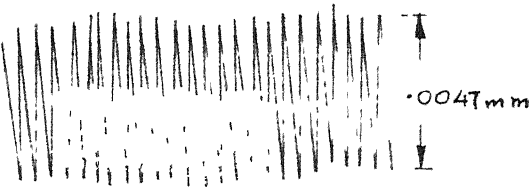
DISPL
↑
TIME →



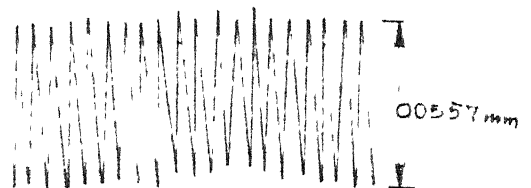
FREQ 220 CPS
(55)



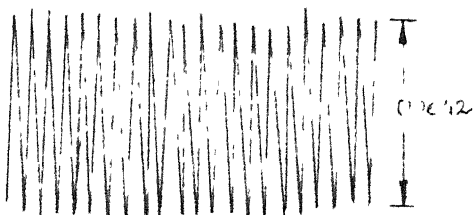
FREQ 200 CPS
(60)



FREQ 230 CPS
(55)



FREQ 190 CPS
(55)



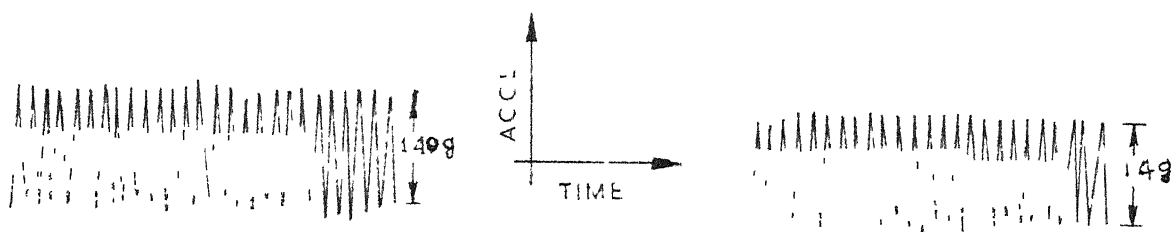
FREQ 200 CPS
(50)



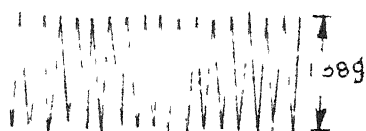
FREQ 170 CPS
(50)

OUTPUT PLATES ARE SHOWN
UNDER BRACKET

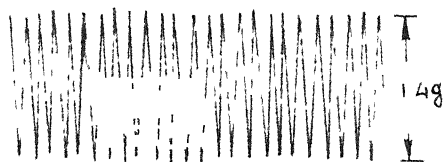
FIG 518 DISPLACEMENT vs TIME RESPONSE



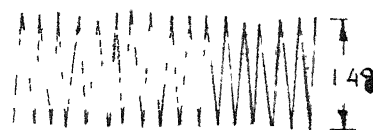
FREQ 250 CPS

FREQ 250 CPS
(output voltage 6r)

FREQ 200 CPS



FREQ 230 CPS



FREQ 190 CPS

FIG 5 19 ACCELERATION VS TIME RESPONSE